The Homogeneous Nucleation Limits of Liquids

C. T. Avedisian

Sibley School of Mechanical and Aerospace Engineering, Cornell University, Ithaca, New York 14853

This work provides a critical compilation of the homogeneous nucleation limits of liquids. Data for 90 pure substances and 28 mixtures have been compiled over a range of pressures, nucleation rates, and compositions. Detailed descriptions of the experimental methods used to obtain the included data are given to assess the accuracy of measured values. Criteria used to select the measurements included in the final listing are discussed.

Key words: boiling; bubbles; droplets; heat transfer; homogeneous nucleation; limit of superheat; metastable states; superheated liquids; vapor explosions; vaporization.

Contents

List of Tables

List of Figures

1. Significance of the Limit of Superheat

The homogeneous nucleation limit, or limit of superheat, of a liquid represents the deepest possible penetration of a liquid in the domain of metastable states. At constant pressure and composition, it is the highest temperature below the critical point a liquid can sustain without undergoing a phase transition; at constant temperature, it is the lowest pressure. The practical significance of this limit resides in the consequences of the phase transition that eventually occurs when this limit is reached. The energy released when a liquid at its limit of superheat vaporizes could create a so-called vapor explosion if a significant fraction of this energy appears in the form of a thermal detonation wave, or if bubbles grow at a rate that exceeds the ability of the surrounding liquid to acoustically respond.[16] Although this energy is orders of magnitude less than that typical of chemical explosions, the destructive capability of vapor explosions produced when a hot nonvolatile liquid comes in intimate contact with a cold volatile liquid is well documented in the literature.[60] It is therefore important to accurately predict the conditions under which liquids can undergo vapor explosive boiling. These conditions involve initiation and propagation mechanisms. The initiation process is relevant to the present study. Subsequent events after the initiation phase involve dynamic and thermal considerations that are outside the scope of this work.

There has been a wide range of opinions offered to explain vapor explosions.[16,60] There is general agreement concerning two necessary conditions:

(1) A volatile and nonvolatile liquid must come into intimate liquid/liquid contact.

(2) The temperature of the nonvolatile liquid must be above some well-defined minimum value (which we shall give the symbol "T_k" in this work) which is at least greater than the boiling point of the volatile liquid: below this threshold temperature, or well above it, vapor explosions may not occur.

Use of this simple threshold temperature criterion requires either a reliable method for estimating T_k, or a listing of measured values. The present work provides such a critically evaluated compilation. It is distinguished from other previous data listings[23,57,82] with respect to the extent of the compilation, the inclusion of data encompassing all pressure and composition ranges, and the criteria used to test the validity of published data. The resulting compilation may be valuable both with respect to its relevance to vapor explosions, and for its more fundamental importance in further characterizing the physical properties of superheated liquids.

2. The Limiting Liquid Superheat as a Physical Property

Normal saturation states of liquids represent a special case of equilibrium across a flat phase boundary. Such equilibrium states are not unique. For example, a liquid that fills a vessel with perfectly smooth walls (the smoothest such walls being the surface of another immiscible liquid) may be heated to temperatures that surpass its "normal" boiling point corresponding to the ambient pressure P_0.

Figure 1 schematically illustrates, on a pressure–temperature projection of a phase diagram, two possible paths that a pure, subcooled liquid may follow to become superheated. The solid line separating the stable liquid and stable vapor regions in Fig. 1 corresponds to phase equilibrium across a flat ($r\rightarrow\infty$) liquid/vapor interface. Transgression of this phase boundary implies an absence of a planar interface between the two phases. Hence, any vapor phase present within the metastable (superheated) liquid region shown in Fig. 1 must be in the form of bubbles ($r<\infty$). The static mechanical equilibrium of such bubbles requires that

$$P + n\cdot P_0 = \frac{2\sigma}{r} > 0 . \qquad (1)$$

For a vapor bubble (when $n\cdot P_0 < 0$), $P > P_0$ and $r < \infty$. Therefore $T(P_0) > T_s(P_0)$, where T_s is referred to $r\rightarrow\infty$. A superheated liquid is one for which $T(P_0) > T_s(P_0)$. There is a limit to the extent to which a liquid can be heated above its normal boiling point (T_s) before a phase transition must occur. The thermodynamic state of a liquid at this theoretical maximum

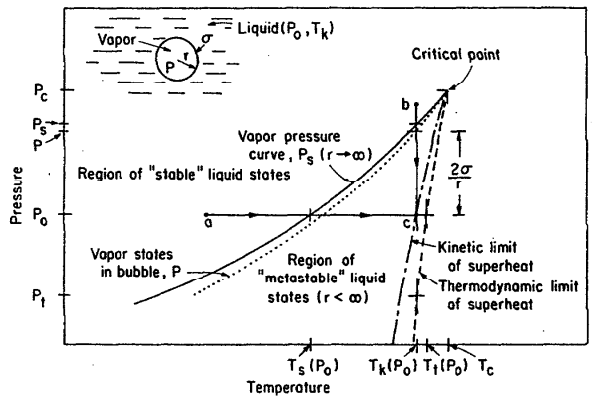

FIG. 1. Pressure–temperature phase diagram for a pure substance (solid/liquid and solid/gas equilibrium boundaries omitted). Path a–c corresponds to isobaric heating. Path b–c corresponds to isothermal decompression.

temperature is on the phase boundary separating the metastable and thermodynamically unstable states. This boundary, known as the spinodal curve, divides stable states from states that are inherently unstable with respect to small perturbations in certain intrinsic variables (e.g., volume along an isotherm for a pure liquid[19]). For a pure liquid the spinodal curve, or thermodynamic limit of superheat (T_t), is defined by states for which[80]

$$\left.\frac{\partial P}{\partial V}\right|_{T,n} = 0, \tag{2}$$

as first presented by Gibbs[41] (the fluid is still stable in the "metastable" regime and is conditionally stable on the spinodal curve). Equation (2) is a consequence of the basic extremum principle of thermodynamics, which states that the entropy is a maximum in a stable equilibrium state. At the limit of stability the second-order variation of the Helmholtz function vanishes along an isotherm, which leads to Eq. (2) for a pure substance. Similar formulations may be developed for multicomponent miscible mixtures of liquids.[19]

The ability to rigorously define in mathematical terms the limit of stability of a liquid supports the belief that it is a fundamental thermodynamic property. It may be considered a kind of "critical point" of a liquid corresponding to each pressure. As such we should be able to experimentally verify its existence and predict it using an appropriate equation of state. It is at this point that we face difficulties.

Firstly, an equation of state applicable in the metastable region is needed to evaluate the terms in the appropriate stability criterion [e.g., Eq. (2) for pure liquids]. Few such equations currently exist. We are therefore forced to extrapolate existing equations of state into the region of metastable states with little data to test the accuracy of such extrapolations; the procedures for such extrapolations are not well developed, although recent work[48] has shown how a cubic equation of state could be used to predict spinodal limits of pure liquids.

Secondly, the limit of intrinsic stability is defined by the entropy-extremum principle. It can therefore only be approached but never actually reached (rather like our inability to precisely reach 0 K). Therefore, if we could accurately predict the limit of stability $T_t(P_0)$, this value would only provide an upper limit on the temperature (or lower limit on the pressure) at which a liquid phase could exist. The best experiments would be expected to yield maximum superheat temperatures T_k (or minimum pressures P_0), such that

$$T_k(P_0) < T_t(P_0). \tag{3}$$

Differences between T_t and T_k are often substantial and outside the range of experimental uncertainty. For example, Table 1 lists predicted thermodynamic limits of superheat calculated using the Peng–Robinson[57] equation of state. Also shown are the highest measured superheat temperatures T_k of the respective liquids. These values were taken from the present compilation (Table 4). The results conform to Eq. (3).

Differences between T_t and T_k can be explained by a physical mechanism for phase transitions, which presumes the existence of microscopic "seeds" or "nuclei" of the vapor phase in bulk liquid. These nuclei are the principal means by which a liquid becomes "aware" of an impending violation of the second law of thermodynamics as the spinodal line is approached. They are postulated to grow or decay in a more or less random manner until a certain size of bubble is produced such that it is in unstable thermodynamic equilibrium with the surrounding liquid. These bubbles are called "critical size nuclei," and their continued growth results in complete vaporization of the metastable liquid.[23,77]

TABLE 1. Thermodynamic limit of superheat of some pure liquids at atmospheric pressure calculated using the Peng–Robinson equation of state

Substance	T_s (K)	T_t (K)	T_k (K)	T_c (K)	T_t/T_c	$J(T_t)$ (nuclei/(cm^3·s))
n-pentane	309	431	426.2	470	0.918	8×10^{24}
n-heptane	372	499	493.7	540	0.924	8×10^{26}
n-octane	399	525	513.8	569	0.923	2×10^{26}
methanol	338	477	466.2	513	0.931	10^{29}
ethanol	352	482	471.5	516	0.934	10^{30}
water	373	596	575.1	647	0.921	9×10^{28}

Kinetic theory provides a means for predicting the birth rate of critical size nuclei. The mean rate of forming these nuclei—effectively, the number of critical vapor nuclei per unit volume and time (given the symbol J)—is proportional to the exponential of their energy,

$$J = \Gamma k_f N_0 e^{-\Delta\Phi^*/kT_k}. \tag{4}$$

Γ is a factor to account for the possibility that nuclei larger than the critical size may decay (assuming that $\Gamma = 1$ introduces little error in predicting T_k) and k_f is a molecular evaporation rate. Solving for T_k, Eq. (4) yields

$$T_k = \frac{\Delta\Phi^*}{k}\left(\ln\frac{\Gamma k_f N_0}{J}\right)^{-1}, \tag{5}$$

where the nucleus energy $\Delta\Phi^*$ is given by the following well-known expression:

$$\Delta\Phi^* = \frac{16\pi\sigma^3}{3(P-P_0)^2}, \tag{6}$$

where[12,23,59]

$$P \simeq P_s \exp\left[\frac{v_l}{RT_k}(P_0 - P_s)\right].$$

From classical homogeneous nucleation theory, one possible expression for the product Γk_f may be derived as[42]

$$\Gamma k_f \simeq \frac{2\sigma}{\pi m}. \tag{7}$$

For a pure liquid, the nucleation rate is then a function of two variables: liquid pressure P_0, and temperature T_k (all physical properties depend on these two quantities, and P_s is only a function of temperature). For a mixture, composition (i.e., mole fraction) must be added as an additional variable.

An alternative interpretation of the nucleation rate is in terms of a waiting time. At a given temperature and pressure, we ask how long one must wait for a critical size nucleus to form in the metastable superheated liquid. In this case,[77] $\tau \simeq 1/(JV)$ where V is the volume of liquid of interest. Table 2 lists calculated waiting times for water under a pressure of 0.101 MPa. Note the characteristic precipitous vari-

TABLE 2. Limit of superheat and nucleation rate of water at atmospheric pressure

T (K)	P (MPa)	P_s (MPa)	$r\times10^7$ (cm)	J (nuclei/(cm^3·s))	waiting time/ cm^3($\sim 1/J$)
500	2.58	2.61	25.2	$<10^{-99}$	$>10^{91}$ yr
550	5.91	6.10	6.76	$<10^{-99}$	$>10^{91}$ yr
560	6.83	7.10	5.2	2.7×10^{-76}	1.2×10^{68} yr
570	7.85	8.2	3.9	8.5×10^{-20}	3.7×10^{11} yr
575	8.39	8.8	3.4	5.7×10^{-3}	1.8×10^{2} s
580	8.96	9.44	2.9	4.3×10^{9}	2.3×10^{-10} s
590	10.16	10.89	2.1	4.3×10^{23}	2.3×10^{-24} s

ation of waiting time (and J) with temperature, though there is a finite nucleation rate corresponding to each temperature. This fact lends some arbitrariness to a precise definition of a maximum liquid superheat based on kinetic theory. By contrast, the thermodynamic limit of superheat [e.g., Eq. (2)] is a well-defined quantity (albeit difficult to predict and impossible to measure). Table 2 shows that, for all practical purposes, intrinsic bubble formation within water is highly unlikely to occur at temperatures below 570 K. Thus the so-called "kinetically" defined maximum temperature, determined by Eq. (5), still represents a fairly well defined limit to the extent to which a liquid may be heated without boiling.

Figure 2 illustrates the qualitative variation of J with T.

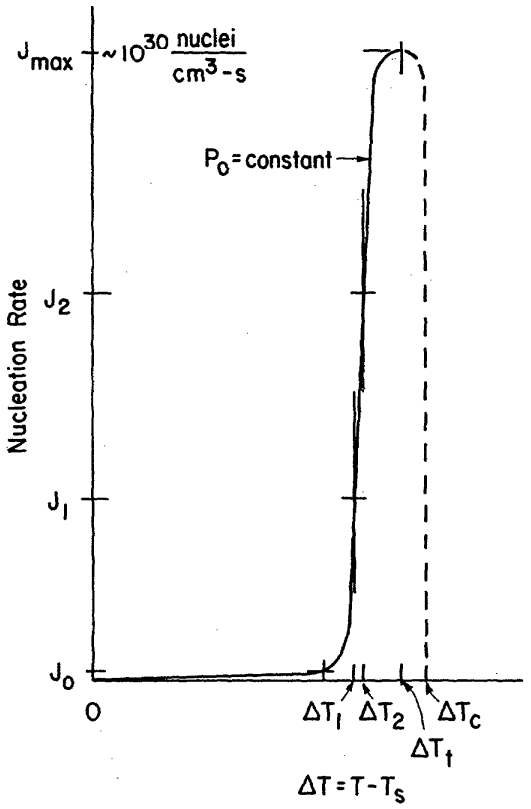

FIG. 2. Schematic variation of nucleation rate with temperature at a given ambient pressure. J_0 defines the minimum nucleation rate below which homogeneous nucleation is unlikely. The superheats ΔT_1 and ΔT_2 correspond to rates J_1 and J_2, respectively. The superheat at J_{max} is shown corresponding to the thermodynamic limit.

Only above a certain (arbitrarily defined) threshold nucleation rate (e.g., J_0 in Fig. 2) is it meaningful to speak of an experimentally accessible limit of superheat. In practice this limiting nucleation rate is defined to correspond to $J_0 \simeq 1$ cm^{-3} s^{-1}. Above this value, the limit of superheat exhibits a small variation with nucleation rate.

An interesting fact that emerges from Eqs. (4)–(7) is that J (for a pure substance) apparently passes through a maximum value at a given pressure P_0 in the temperature range $T_s < T_k < T_c$. This result follows because $J\to0$ ($\Gamma k_f \to 0$) as both $P\to P_0$ (i.e., along the "normal" saturation curve) and $T_k \to T_c$. It is attractive to suppose that the temperature corresponding to this maximum value of J lies on the spinodal curve. Lienhard and Karimi[49] have conjectured this to be the case. They have estimated a maximum universal nucleation rate of about 10^{28} cm^{-3} s^{-1}. Pavlov and Skripov[56] estimated this maximum to be about 10^{30} cm^{-3} s^{-1}. Table 2 lists values of J calculated at T_t using Eq. (4). The results conform to the above ranges. (It is questionable whether such high rates could ever be achieved in experiment.)

If the calculated variation of J with T and P_0 obtained from Eq. (4) is indeed correct, then measured values of T_k obtained from various experimental methods must be less than the thermodynamic limit of superheat at the same pressure—Eq. (3) must be satisfied. Unfortunately, the inability to accurately predict T_t eliminates the potential usefulness of this fact as an aid for testing the validity of purported superheat limit measurements.

3. Experimental Methods

This section reviews the most often used methods for measuring the limits of superheat of liquids. All the data included in Tables 4–6 were taken with one or more of these methods.

3.1. Methods Involving Liquids in Contact with Solids

a. Introduction

The high liquid superheats characteristic of homogeneous nucleation are generally difficult to reach when a liquid is in contact with a solid. Vapor formation may be initiated by nucleation of gas bubbles at the solid/liquid interface (heterogeneous nucleation) at superheat conditions much less extreme than for homogeneous nucleation. The energy of bubble formation at a flat smooth surface is less than for bubble formation in the bulk of a liquid at the same ambient pressure. The corresponding superheat is thereby generally reduced[77] (though the competing influence of reduced number density of molecules at a surface relative to the bulk could lead to a higher probability for bubble nucleation in the bulk depending on the contact angle[82]). Yet, in spite of these facts, two principal methods for measuring the superheat limit of liquids have emerged which involve liquids in contact with solids. These methods have produced superheat limit data that are, in some cases, quite close to values predicted by homogeneous nucleation theory, Eqs. (5)–(7). Data from some of these methods are therefore included in the present compilation.

The principles of these methods are discussed to show

why measurements obtained from them may qualify as valid superheat limits. Two successful methods have involved (1) rapidly heating a wire or flat crystal immersed in a subcooled pool of the test liquid—the so-called pulse heating method[26,56,64,65,72,75,77] and (2) isothermally decompressing[14,28,29,37,44,66–68,76,83] or isobarically heating[15,30,34,47,53,74] a small volume of liquid in a container, which may be a capillary tube made of glass or metal.

b. Pulse Heating Method

One variant of the pulse heating method consists of imposing a programmed current ($\sim$10 A) through a small diameter platinum wire ($\sim$0.02 mm in diameter and 1.0 cm long). During the time of application of the current (ranging between 25 and 1000 μs), the wire heats the liquid adjacent to it, thereby creating a thermal boundary layer around the wire. When the liquid in this boundary layer reaches the superheat limit, bubbles appear and alter the wire resistance by their effect on the heat transfer between wire and liquid. This resistance change may be measured, thereby giving a measure of the liquid temperature at which bubbles are formed. The wire thus acts as both a temperature sensor and a heat source.

The wire diameter and the magnitude and duration of the imposed current are chosen so as to minimize the tendency of the wire to promote nucleate boiling from gases trapped in surface defects of the wire. The idea is to heat the wire at a sufficiently high rate for a short enough time that any bubbles that would tend to grow and detach from the wire would require a longer interval of time than is necessary to heat the liquid around the wire to its limit of superheat. The bubbles that do form create a measurable temperature perturbation of the wire by their effect on the heat transfer between the wire and the surrounding liquid. This temperature perturbation ($\sim 10^{-3}$ K for most organic liquids) may be related to the nucleation rate.[77]

Few details have appeared in the literature that permit results obtained from this method to be reproduced and that allow accurate estimation of the errors involved. The pulse heating method of using a wire as the heating element has apparently been successfully employed only by Skripov and co-workers[56,72,75,77] and Sinha,[64] while another study[58] attempted to reproduce the method without much success. A variant of this method involved rapid heating by a pulsed current of a bismuth crystal immersed in a bath of the test fluid.[26,64,65] This method was successfully used to measure the limit of superheat of helium I. The bismuth crystal served both as the heating element and temperature sensor by the strong dependence of its magnetoresistance with temperature. The low contact angle and surface tension of helium I ensured a negligible influence of the crystal on surface nucleation.

The errors associated with the pulse heating method are (1) spatial nonuniformities in the heating element temperature (the temperature inferred from its resistance is an average characteristic of the entire heated element mass), (2) reproducibility in the calibration to relate element resistance with temperature, (3) pressure changes in the liquid film surrounding the element, due to abrupt thermal expansion on bubble formation, and (4) measurement of the temperature perturbation created by bubble nucleation. The cumulative error in the superheat limit associated with the first three effects has been estimated to range between 10^{-3} and 5 K.[26,65,72,75,77] Temperature perturbation and bubble density measurement errors are much less important. This information is used to estimate the nucleation rate commensurate with the imposed current pulse and ambient pressure.

c. Capillary Tube Methods

Isobaric Heating

The original experiment of this genre was performed by Kenrick *et al.*[47] The method consists of heating liquid-filled glass capillary tubes in a constant pressure environment. The purpose of using capillary tubes is to reduce both the number of potential nucleation sites by reducing the liquid/solid contact area, and the size of these sites. The liquid is brought into the metastable state along path a–c in Fig. 1. At a certain characteristic temperature, usually identified with the homogeneous nucleation limit, the liquid in the capillary boils. The nature of this boiling depends on the ambient pressure. At pressures near atmospheric, most hydrocarbons characteristically "explode" in the capillary. This explosive boiling is usually manifested by an audible sound, such as click or crack. At elevated pressures, generally above 0.5 P_c,[74] boiling loses its explosive character. Measurement of the superheat limit then relies more heavily on visual observation (bubbles in the capillaries are observable), and any temperature and pressure perturbations produced by the phase transition. The corresponding accuracy of the measurement thus appears to be reduced at higher pressures.

Three major sources of error associated with this method are (1) minimizing the effect of the container walls (the capillary tube surface) on promoting heterogeneous nucleation at the liquid/glass interface, (2) the thermal lag between the test liquid and surrounding heat bath, and (3) spatial nonuniformities of temperature within the superheated liquid sample.

The effect of solid/liquid contact resides in the propensity for the solid to (1) reduce the energy required to form a critical size bubble at the solid/liquid interface and (2) trap noncondensable gases in surface irregularities. The former effect may be minimal depending on the glass/vapor/liquid contact angle. The latter effect is more serious in that it is difficult to create a hypothetically smooth (on a microscopic level) surface, and to remove gases trapped in surface irregularities. These effects may be minimized, however, by reducing the volume of liquid heated, carefully cleaning the test surfaces, prepressurization, and degassing the test liquids. The fact that liquids have been heated to values within a few degrees of their theoretical limits of superheat is testimony to the value of these preparatory efforts. The number of studies that have been successful in this regard is, however, small. Efforts were made to select from among the large number of studies that used capillary tubes for measuring the superheat limit, those that yielded superheat temperatures that appeared to characterize the intrinsic nature of the liquid itself, rather than the adhesion of the liquid to its container.

Systematic errors are created by the thermal lag

between the test liquid in the capillaries and the heat bath within which the capillaries are heated (which may be a thermostatted liquid pool[34,47,53] or thermostatted solid block[15,74]), and heat conduction effects through the walls of the capillaries themselves. To reduce the temperature difference across the capillary, the heating rate (dT/dt) should be low and the capillary wall thickness small. Typical experimental values have ranged between 0.01 and 3 K/s, and between 0.07 and 1 mm. Spatial nonuniformities of T_k are reduced by superheating small liquid volumes. Values have ranged between 0.01 and 0.1 cm^3. A rather simple lumped capacity model of the volume of superheated liquid, together with assuming a linear variation of T at the above mentioned values, can be shown to yield temperature underheatings of the test liquid on the order of less than 1 K.

Isothermal decompression methods

(a) Bubble chambers

Another path for transgressing the phase boundary of a liquid (besides isobaric heating) is isothermal decompression (path b–c in Fig. 1). Experimental techniques that have utilized this idea are called "bubble chambers."[14,28,29,37,44,66–69,83,85] A forerunner of this method was originally developed by Wismer[85] in 1922. One end of a sealed capillary tube containing the test liquid (ethyl ether, isopentane, or ethyl chloride) was connected to a screw-type cylinder, which was used for pressurizing the test liquid. The capillary was placed in a thermostatted reservoir, and the pressure was initialized to a value greater than the saturation pressure corresponding to the reservoir temperature. Suddenly releasing the pressure brought the initially subcooled ($P_0 > P$ in Fig. 1) test liquid into the metastable state. Vaporization was usually manifested by an audible sound after a certain waiting time. Subsequent refinements to the method consisted of improving accuracy of pressure and temperature measurement, correcting for, and minimizing, the temperature drop associated with the idealized adiabatic decompression process, and refining the measurement of waiting time and the detection of vaporization itself in the capillary.[14,28,29,37,66–69,83]

Data obtained from this experiment are the ambient pressure P_0, superheat temperature T_k, and the waiting time τ. In a certain temperature range, the waiting time is observed to abruptly decrease with a comparatively small increase in temperature. For example, at only 2.5 K below the mean limit of superheat of several organic liquids, the waiting time was found to decrease from over 1 h to just a few s.[67] This behavior is indicative of a homogeneous nucleation phenomenon and is a manifestation of the very strong dependence of nucleation rate on temperature. The mean temperature in this range of sudden change in τ is identified with the limit of superheat corresponding to a nucleation rate associated with τ (see Sec. 4). Measurement of temperature and waiting time in the region of T_k is the intent of the experiment.

Systematic errors of the method are due to (1) the temperature drop of the test liquid during adiabatic decompression, (2) propensity for nucleation to occur on the walls of the capillary (this problem also occurs, to a lesser extent, with the pulse heating method), and (3) spatial nonuniformities of temperature in the volume of superheated liquid. For mixtures, accuracy of the mixture composition may also be problematic, though composition errors on the order of only 0.1 mol % are typical.[29]

The small temperature drop of the test liquid caused by rapid decompression was kept to under 0.5 K by a two-stage decompression technique. Spatial nonuniformities of temperature within the test volume were also minimized by using small volumes. Typical values have ranged between 0.005 and 0.15 cm^3.[14,29,67–69] Small-diameter tubes also minimize the effect of gas bubble nucleation from gases trapped in surface irregularities. An exception is the experiments reported by Hord *et al.*[44] on superheating liquid hydrogen. The hydrogen pool chamber volume was nearly 1000 cm^3, yet their data are indicative of the limit of superheat of hydrogen. The reason relates more to the test fluid properties than to any special liquid or container preparation techniques. The surface tension and wetting characteristics of liquid hydrogen at low temperatures—25 to 30 K—are such that the presence of vapor-filled cavities is unlikely. With no potentially active surface nucleation sites, the liquid superheat is limited by the type of random density fluctuations that lead to homogeneous nucleation.

(b) Dynamic Stressing Method

Dynamic stressing methods bring subcooled liquids into the metastable state by isothermal decompression (path b–c in Fig. 1). Differences with the bubble chamber technique reside in the method of stressing the liquid, and the pressure and temperature ranges at which vaporization is induced. Temperatures at the start of decompression are typically low enough that the pressure on the liquid changes from a compressive to a tensile stress (path b–c in Fig. 3). This gives rise to the concept of "negative pressure."[20,21] This term is used to identify the direction of the imposed pressure on the liquid relative to the outward normal on the nucleus surface. Figure 3 illustrates the concepts involved.

The static mechanical equilibrium of critical size nuclei requires that Eq. (1) be satisfied. Given that $n \cdot P \equiv P$ will always be positive, a liquid temperature—T' (Fig. 3)—exists below which the liquid pressure will be extensive relative to the nucleus surface ($n \cdot P_0 > 0$), and above which it will be compressive ($n \cdot P_0 < 0$). Dynamic stressing methods usually operate in the temperature range for which $T < T'$ (in fact, usually $T_r < 0.7$ in contrast to other experimental methods in which $T_r > 0.9$ when $T > T'$). Furthermore, most reported data are such that $|P_0| \gg |P|$ so that the "tensile strength" P_0 is related to bubble radius as

$$P_0 \simeq \frac{2\sigma}{r}. \tag{8}$$

Equation (8) is typical of cavitation induced nucleation. By convention, measured nucleation pressures are assigned negative values when $T < T'$ ($n \cdot P_0 > 0$).

Three types of experiments have been developed to measure the tensile stress (i.e., negative pressure) of liquids. The first involves static application of tension to a liquid. The second involves dynamically stressing the liquid, and

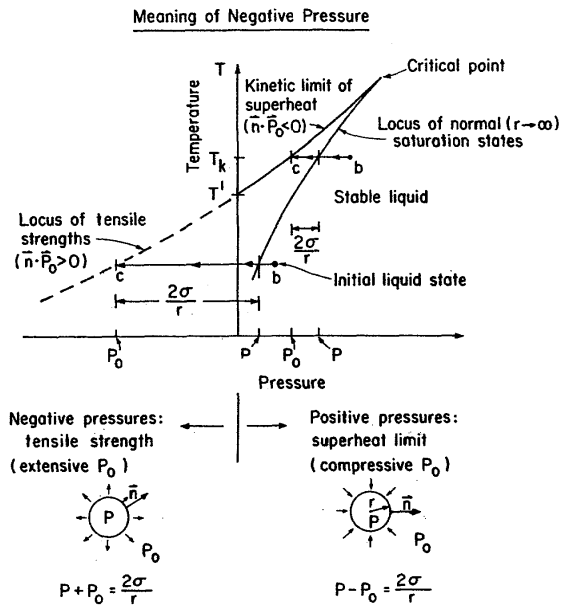

FIG. 3. Schematic illustration of states corresponding to the tensile strength (i.e., limiting negative pressure). When $T>T'$ ambient pressure is compressive. When $T<T'$ ambient pressure is extensive.

the third method concerns imposing ultrasonic waves of high amplitude on the test liquid.

(1) Static application of tension to a liquid was first employed by Berthelot[20]—the so-called "Berthelot tube method." In this technique, a tube, typically a glass capillary or steel tube, is almost completely filled with the test liquid. The remaining volume is occupied by air. With the tube sealed, the contents are heated and the trapped gas is forced into solution. Subsequent cooling contracts the liquid, and the difference between the expansion coefficients of the liquid and material that encapsulates it creates a state of internal stress in the liquid, the liquid essentially attempting to contract more than its solid container. Eventually the contraction tears the liquid from the walls of its container and the liquid "ruptures." The breaking pressure may be evaluated from either the increase in volume of the container caused by the phase change (if the container walls are flexible)[81] or the volume of the vapor produced in the container.[77] In the original work of Berthelot, the tensile strength of water was measured at room temperature to be about 5 MPa. More recent work[46] in which one side of the tube wall formed the surface of a pressure transducer reported a limiting tensile stress for water at 279 K of 4.66 MPa. Considering that the theoretical values of the limiting negative pressure for water in a temperature range of 273 to 373 K have been estimated to vary from about -100 to -600 MPa, there is serious doubt concerning the identification of these data with the true tensile strengths of water. Even accounting for the effect of dissolved gases in the test sample cannot bring theory and experiment into agreement. This fact suggests that what may be really measured in this static stressing method is the adhesion of the liquid to its container, rather than the intrinsic adhesion of the liquid to itself. For these reasons, nearly all data obtained from static stressing methods of the type described above have been rejected in this compilation. (See Sec. 5.2 for exceptions.)

(2) Dynamic stressing methods are similar to the Berthelot tube method except that a state of tension is now induced by centrifugal rotation or sudden linear deceleration of the test liquid.[8,18,24,25] A Z-shaped tube used by Briggs[24,25] (0.6 to 0.8 mm internal diameter) was rotated about its z axis. One half of the liquid in the tube thereby pulls against the other half at the center of rotation, and the maximum stress occurs at the tube center. At a certain rotational speed the liquid in the tube center will fracture—literally split apart. (This method is qualitatively similar to that discussed by Trevena[81] in which a shock wave was generated in a liquid by firing a bullet against a steel tube fitted with a piston at one end. The rarefaction wave generated by reflection of the shock wave created tension in the liquid which subsequently led to its rupture.) The breaking stress may be related to the angular velocity of the tube. Maximum tensile strengths for water thus far reported—27.5 MPa at 281.2 K[25]—are still far below theoretical estimates. As with the Berthelot tube method, measured fracture pressures are probably indicative of the adhesion strength of the test liquid to its container walls. Nevertheless, these data are the best available measurements and are included in Table 4 so as to provide a basis for comparison with future work. A refinement of this method by Apfel[8] involved greater care in preparing the test liquid (i.e., prestressing it) and using a test fluid with a lower surface tension (ethyl ether).

The linear deceleration method employed by Beams[18] utilized an inverted U-shaped capillary tube (3–5 mm internal diameter) which was thrust downward and then abruptly stopped. The downward momentum imparted to the liquid by this sudden stopping action created a tensile stress in the upper portion of the tube, which essentially "broke" the liquid. The tensile strength was then inferred from the height of the liquid in the arms of the U tube, the temperature, and the deceleration force. Values of tensile strength for several cryogenic liquids again exhibited serious discrepancies with nucleation theory. The reported negative pressures are therefore not indicative of having reached the true limit of superheat. Nevertheless, the reported tensile strengths are the best available data and are therefore included in Table 4 for completeness.

(3) One of the most successful methods for measuring the limiting negative pressures of liquids was developed by Apfel.[3–6] The technique involved levitating a test liquid droplet by a standing wave field generated by a piezoelectric acoustic transducer cemented to the walls of a vertical tube filled with another immiscible liquid (similar to the bubble column method—Sec. 3.2.a). The droplet is stressed for those periods it is exposed to the negative parts of the acoustic cycle. When the magnitude of the negative pressure is high enough and of long enough duration, any cavities formed by homogeneous nucleation will grow to observable size. This growth is usually manifested by an explosive type of boiling, depending on the pressure level. (If the cavity does not grow fast enough during the negative part of the cycle, it will collapse as the acoustic pressure becomes positive.) The excellent agreement between measured negative pressures

and values calculated from homogeneous nucleation theory, e.g., Eqs. (5)–(7)—the first such agreement yet demonstrated for the tensile stress of a liquid[4–7]—is evidence that the problems that prevented such agreement using the other methods described above were largely overcome by this variant of the floating droplet method. Tensile strength measurements obtained from this acoustic levitation method are therefore regarded as indicative of the true tensile strength of the test liquids. A similar method was used by Marston[50] to measure the extent of superheating of helium II (the helium was now in contact with the walls of a thermostatted bath). The poor agreement between measured and calculated values (at 2.09 K, calculated tensile strengths ranged between -0.3 and -0.5 MPa, whereas the measured value was -0.06 MPa) may be more indicative of inaccuracies in predicting the physical properties of helium II (in particular, surface tension) than to defects in the experimental method. These measurements are inconsistent with those reported by Beams,[18] but are believed to be more reliable owing to direct observations of bubbles nucleating within the bulk of the stressed helium II pool.[50]

d. Bulb Method

In this method, a heated surface (a spherical glass bulk) is placed in a pool of the test liquid. The test liquid adjacent to the bulb then becomes superheated and eventually boils. The vaporization temperature is measured by measuring the bulb wall temperature (due account being taken of the temperature drop across the bulb wall). Boiling is typically detected by the visual appearance of bubbles on the bulb surface.

The rather large size of heated surface which is in contact with the test liquid (the bulb was 2.1 cm in diameter[17,63]) increases the probability for gas bubble nucleation on the surface. This fact is reflected by the comparatively low superheats realized by this technique in comparison with those measured using other methods. For example, the maximum liquid temperature before vaporization of *n*-heptane at 0.101 MPa was measured to be 430 K. This value is more than 50 K below the true limit of superheat of *n*-heptane (see Table 4). Even neglecting the (rather substantial) temperature drop across the bulb cannot reduce this discrepancy. Similar discrepancies may be noted for the other fluids tested in Refs. 17 and 63. Most of these data were therefore not included in the final listing.

The few data which were included from Refs. 17 and 63 are the highest temperatures to which the respective liquids have been heated before undergoing a phase change. These superheat temperatures, however, are not indicative of the true limit of superheat. Future work on these substances may use the included data as base values above which the respective superheat temperatures must fall.

3.2. Methods Involving Liquids in Contact with Immiscible Liquids

a. Introduction

These methods consist of suspending a volatile droplet of a test liquid in another nonvolatile liquid (the "field" liquid) in which it has a low solubility. The field liquid is then subjected to such conditions as to bring the encapsulated droplet into the metastable state. These conditions have consisted of isobarically heating the field liquid[1,2,11–13,22,35,36,42,52,54,55,59,61,62,71,73,77–79,84] or isothermally decompressing it.[3,10,38–40,51] The corresponding states that the test droplet experiences as it approaches its limit of superheat are illustrated by paths a–c and b–c, respectively, in Fig. 1. When the test droplet vaporizes, the ambient pressure and temperature at which this boiling takes place are inferred from corresponding measurements in the field liquid. Principal errors associated with the method are, therefore, discrepancies between the field and test liquid temperature and pressure. Pressure differences are negligible. However, the average droplet temperature, both spatially and temporally, may be quite different from the field liquid, the extent of the difference depending on the droplet size and other factors as discussed below.

The chief advantage of the floating droplet method over other methods involving encapsulation of the test liquid in a solid container (i.e., pulse heating or capillary tube methods) resides in the fact that the test droplet/field liquid interface constitutes a hypothetically ideal smooth surface, free of any solid motes or trapped gases which would tend to initiate a phase transition. The liquid/liquid interface has essentially a similar microscopic structure to the bulk of the droplet. Any phase transition at this interface would therefore have to occur by the same mechanism as in the bulk of the test droplet. Depending on the surface and interfacial tensions of the test and field liquids, the probability for homogeneous nucleation may be greater in the bulk of the test droplet (desired) than at the liquid/liquid interface (undesired). The key to successful use of this method therefore relies on carefully selecting the test/field liquid combination to satisfy the following criteria: (1) the field liquid must have a boiling point higher than the limit of superheat of the most nonvolatile component within the test droplet over the entire range of ambient pressures at which the limit of superheat is to be measured, (2) both liquids must have low mutual solubility, (3) the physical properties of both liquids should be available (or predictable), and (4) the probability for nucleation within the bulk of the test droplet must be higher than that at the droplet/field liquid interface. The last requirement is satisfied if[7,9,23,45,51]

$$\sigma_2 > \sigma_1 + \sigma_{12}\,, \tag{9}$$

where σ_1, σ_2, and σ_{12} are surface tensions (against their own vapor) of the test liquid (1) and field liquid (2) and interfacial tension (12), respectively. If Eq. (9) is not satisfied, measured superheat limits will essentially have characterized the interface between the two liquids rather than the test liquid itself (similar to the situation which occurs for some of the isothermal stressing methods described in Sec. 3.1.c). The measured temperatures (at a given pressure) will, in this event, be generally far below what would be indicative of homogeneous nucleation in the bulk of the test droplet.[10,23,45] This fact limits the extent of the various liquids which can be tested by floating droplet methods. Nevertheless, the method, when the above criteria are satisfied, has yielded some of the most reproducible and accurate superheat limit data thus far reported.

b. Isobaric Droplet Heating

The first experimental proof of the existence of superheated liquids was obtained by Dufour,[31,32] who heated water droplets of 1–2 mm diameter in a pool of oil of roughly equal density. On slowly heating the oil, the water droplets were able to sustain temperatures as high as 448 K before boiling. The phase change was always observed as a violent explosion in these tests. Though this temperature is low compared to more recently measured values,[2,22] Dufour's experiments were remarkable for their day. They remained the highest measured liquid phase temperatures for water at 0.101 MPa for over 100 years.

The modern adaptation of Dufour's method consists of injecting small light volatile droplets (0.1–1 mm) of a test liquid into the bottom of a vertical tube (called a "bubble column") that contains a heavier immiscible nonvolatile field liquid. A stable temperature gradient is imposed on the field liquid such that temperature is hotter at the top of the column than at the bottom. As the droplets rise, they are progressively heated until they begin to boil. This boiling may either take the form of a small explosion (audible as a cracking sound) or a sudden increase in rise velocity of the droplet caused by a bubble growing inside the droplet, depending on the ambient pressure and composition of the droplet. The droplet vaporization temperature and pressure are inferred by measuring the temperature and pressure in the field liquid at which vaporization occurs.

This method has become very popular because (1) the experiment is quite simple to construct and operate, and (2) the measured superheat limits essentially agree with the theoretical predictions of homogeneous nucleation theory.

The bubble column itself is glass with inside diameters that have ranged from as small as 1.3 cm[11] to over 6 cm.[62] Tube length has ranged from 100 cm[1] down to 35 cm.[73,84] Temperature gradients imposed on the field liquid have been effected by heating Nichrome wire wrapped around the tube with varying pitch.[1–3,22,33,42,52,54,55,59,61] Other approaches have employed a metal sleeve fitted around the tube with attached electrical heater[13,35,36,62,71,73,78,84] and a commercially available rope heater.[11] Temperature gradients produced by these various methods have ranged from 0.03[42] to 10 K/cm.[71] For typical rise velocities in the range of 1 to 5 cm/s, test droplets are heated at rates ranging from 0.03 to 50 K/s.

Field liquids that have been used as heating media include: glycerine; ethylene glycol; sulphuric acid; various mixtures of water with ethylene glycol, lithium chloride, and ammonium; Krytox 143AD (Dupont); benzyl benzoate; and silicone oil. Superheat limits measured using different field liquids (for example, pentane droplets in both glycerine and sulphuric acid) have yielded no discernible differences. This would confirm that measured vaporization temperatures in these cases characterize the test liquid and not the test/field liquid interface.

Principal errors associated with this method are due to underheating of the test droplet caused by a finite heat transfer rate between the droplet and ambient liquid, spatial nonuniformities of droplet temperature, heat conduction along thermocouple wires, and finite solubility between test droplet and field liquid. Detailed modelling of the first three effects has shown that for droplets less than 1 mm in diameter, the droplet surface temperature is within 2 K of the ambient.[73,77,79] For smaller droplets, the errors are much less (viz., 0.6-mm droplets typically lag the ambient temperature by 1 K,[79] while 0.3-mm droplets are typically only 0.1 K cooler than the field liquid[73]).

More serious difficulties are encountered when the droplet and field liquid are not completely immiscible. This effect is usually observed as the test droplets decreasing in diameter as they move through the bubble column.[42,79] The droplet, then, essentially becomes a mixture of a volatile and nonvolatile liquid. The corresponding limit of superheat will then be higher than what would be realized for a completely immiscible droplet/field liquid combination. This superheat limit is no less valid than the superheat limit of the test liquid itself. The difficulty is in knowing to what precise composition this superheat limit corresponds. These problems are encountered with nearly all test/field liquid combinations. This ambiguity is most pronounced for very small droplets (< 0.1 mm in diameter): droplets of this size may completely disappear as they are heated to temperatures approaching their limits of superheat. Larger droplets are better able to survive before completely dissolving, but the problem of droplet underheating then increases.

As a droplet dissolves, a diffusion front will propagate inward from the droplet surface. The central region may be assumed undisturbed at the original composition until the diffusion front reaches the droplet center. During this time the composition will vary from pure test liquid to pure ambient liquid. The limit of superheat will range from a value corresponding to the pure test liquid to that corresponding to the field liquid. The region in this diffusion zone most likely to reach its limit of superheat first is the diffusion front. Thus, even in the presence of appreciable dissolution, measured droplet vaporization temperatures may be characteristic of the test liquid itself. All of the data reported in Table 4 obtained by the bubble column method have yielded temperatures that are within a few degrees of the best estimates of the superheat limits of these substances. The strong dependence of nucleation rate on superheat limit (Sec. 4) together with the above noted agreement, is strong evidence that the true limits of superheat were measured in these experiments.

The situation for miscible mixtures of liquids is more tenuous. The relative rates of diffusion of the various components into the field liquid make it difficult to know the precise composition of the droplet. For equal rates of diffusion, the situation would be as described above for pure liquids. For unequal rates, the composition of the liquid undergoing homogeneous nucleation would be unknown, thus rendering any measured droplet vaporization temperatures meaningless. Those data listed in Table 5 taken using the bubble column method apparently had low enough mutual solubility of all components in the respective field liquids that measured superheat limits were found to be within a few degrees of predicted values. Solubility effects for these data are thus considered to be minimal (at least compared to errors created by droplet underheating).

c. Isothermal Decompression Methods

The isothermal decompression method is essentially the same as the bubble column technique described in the previous section. The main difference is that the field liquid temperature remains isothermal while the ambient pressure is reduced. Encapsulated droplets thus become superheated by following path b–c in Fig. 1.

This method eliminates the problem of droplet underheating because the droplets may, in principle, be levitated in the isothermal field liquid for such time as is required for thermal equilibrium to be established. Larger droplets may also be studied, thus reducing the solubility problem noted in the previous section. The method is also convenient for measuring the limits of superheat of test liquids that are heavier than the candidate field liquids (e.g., the Freon 12/water system studied by Moore[51]). In this case, the droplets must be introduced into the top of the bubble column. During their transit down the column, they are superheated by reducing the pressure on the field liquid.

Experimental difficulties associated with isothermal decompression methods are more formidable than the simple isobaric bubble column. The isothermal bubble column must be pressurized. The test liquid droplet must then be introduced into this pressurized atmosphere and remain there until thermal equilibrium is established and the pressure is reduced from its initial value ($P_0 > P$) to the final nucleation pressure ($P_0 < P$). Three variants of this method have been employed: (1) acoustic levitation of the test droplets,[3–6] (2) droplet levitation in an isothermal flow field,[38–40,43] and (3) droplets freely falling in an isothermal bath of the field liquid.[10,51] Droplet levitation methods are attractive for both measuring the nucleation pressure of the test liquid as a function of field liquid temperature, and studying the intensity of vaporization of the motionless droplets.[5]

Principal errors associated with isothermal decompression methods are fewer than isobarically heating the droplets. The droplets are essentially isothermal. No positioning difficulties of thermocouples at the location of droplet boiling exist because of the isothermal conditions in the field liquid. Typical errors in pressure measurement are identifying the pressure on the field liquid during decompression at which the droplets vaporize. This difficulty can be minimized by slowly reducing the pressure (e.g., a few kPa per s), and recording the pressure transient on a chart recorder with an event marker to identify the correct nucleation pressure. In those cases where vaporization is sufficiently violent, the pressure perturbation produced in the test section as a result of the droplet undergoing homogeneous nucleation may be large enough to be detected by the pressure sensors.[38–40] Errors in nucleation pressure measurement have thus been reported to range from a few percent to about 10%. Since the limit of superheat has a rather small dependence on pressure compared to the effect of temperature on the nucleation pressure (as shown by the data in Tables 4 and 5) errors in nucleation pressure are much less important than errors in the limit of superheat at a given pressure. The uncertainty in nucleation pressure noted above is therefore insignificant.

4. Nucleation Rates Commensurate with Experimental Conditions

4.1. Introduction

For the limit of superheat of a liquid to be meaningful, it is necessary to know the approximate nucleation rate to which it corresponds. Equation (5) by itself is indeterminate without added information which could be used to independently arrive at an estimate of J. Fortunately, the very weak dependence of T_k on J (Fig. 2)—J occurs in a logarithmic term in Eq. (5)—relaxes requirements for an accurate estimate of J. The superheat limit may be shown to change by little more than 1 K for a three to four order of magnitude change in J.

In this section we present very approximate formulations for the nucleation rate appropriate to the various experimental methods that have yielded valid superheat limit data. These formulations are based largely on physical insight. They are believed to be indicative of the orders of magnitude of nucleation rates one may expect to achieve in the various experimental methods considered.

4.2. Floating Droplet and Capillary Tube Methods

The main differences between these two methods are in the volume of liquid heated, the rate at which the liquid is brought into the metastable state, and the container within which the test liquid is heated (solid walls for the capillary tube method and a liquid/liquid interface for the floating droplet method). In other respects an estimate of the nucleation rate may be derived in an equivalent manner for the two methods.

From the meaning of the nucleation rate, the total number n of critical size nuclei produced in a volume V in the time interval 0–τ is

$$n = \int_0^\tau JV\,\mathrm{d}t\,. \tag{10}$$

Two approximate means for estimating J from Eq. (10) are now considered.

The first approach assumes that the volume of liquid V is brought into the metastable state such that J behaves like a delta function but with a finite value at τ. At time τ, a number n of critical size nuclei form at the rate J. Equation (10) can then be written

$$J \simeq \frac{n}{V\tau}\,. \tag{11}$$

Now by convention[34,61,77] we will define the nucleation rate to correspond to only one nucleus forming in the volume V. This assumption can never be proven because of the inability to observe the events leading to formation of critical size nuclei. These events occur on a microscopic scale. However, recent photographic evidence of bubble formation in pure liquid droplets has revealed only one bubble within the droplet.[62] Thus we will take $n = 1$. Equation (1) then becomes

$$J = \frac{1}{V\tau}\,. \tag{12}$$

[Equation (12) was used to calculate the waiting times shown

in Table 2.] Equation (12) may be used to provide an estimate of the nucleation rate commensurate with those experiments in which τ may be measured directly, and the volume of superheated liquid is well defined (e.g., as in the capillary tube and floating droplet methods if τ can be reasonably estimated[42]). In other cases, it is more convenient to account for the variations of J with T as the liquid state transgresses its phase boundary. This leads to a second approach for obtaining an estimate of nucleation rate from Eq. (10).

The continuous variation of nucleation rate with temperature should be considered in evaluating the integral in Eq. (10). This is done below for the case of a constant heating rate and a constant decompression rate.

For a constant heating rate it is convenient to change the variable of integration from t to T through the relation $\dot{T}\,dt = dT$. Equation (10) then becomes (with $n = 1$)

$$1 = V\dot{T}\int_{T_o}^{T} J\,dT\,. \tag{13}$$

Now in the temperature range of interest, it can be shown that Eq. (4) is well approximated by the following relation[77]:

$$J \simeq e^{-G_T(T-T_o)}, \tag{14}$$

where T_0 is chosen as the temperature where $J = 1$ nucleus/cm^3·s (this choice is arbitrary and selected only for convenience), and $G_T \equiv d(\Delta\Phi^*/kT)/dT$ and is approximately constant over the temperature range T_0 to T. Combining Eqs. (13) and (14) and integrating gives

$$J \simeq \frac{|G_T|\dot{T}}{V}\,. \tag{15}$$

Equation (15) is useful for estimating the nucleation rate corresponding to an experiment in which the volume and ambient pressure are fixed, while the test liquid is heated at the rate $\dot{T}$.

For isothermal decompression techniques, Eq. (15) is awkward to use. Decompression causes a temperature drop in the test liquid due to its finite adiabatic compressibility. In this event the magnitude of the heating rate may be expressed as

$$\dot{T} = \frac{dP_0}{dt}\cdot\frac{dT}{dP_0}, \tag{16}$$

where dT/dP_0 may be measured. Equation (15) then becomes

$$J \simeq \frac{|G_T|\cdot\dot{P}_0\cdot dT/dP_0}{V}\,. \tag{17}$$

The decompression rate $\dot{P}_0$ is fixed by experimental conditions.

A nucleation rate commensurate with the floating droplet and capillary tube methods may now be estimated from Eqs. (15) and (17), respectively. For the isobaric heating variant of the capillary tube method, we have the following information

$$0.01\ \text{K/s} < \dot{T} < 3\ \text{K/s}$$

and

$$0.01\ \text{cm}^3 < V < 0.1\ \text{cm}^3\,.$$

Equation (15) then gives

$$1\ \text{nucleus/(cm}^3\text{·s)} < J < 10^3\ \text{nuclei/(cm}^3\text{·s)}\,. \tag{18}$$

For the isothermal variant of the capillary tube method (i.e., bubble chamber experiments), best estimates from available information give[68,69]

$$dP_0/dt \simeq 1.01\ \text{MPa/s}\,,$$

$$dT/dP_0 \simeq 0.5\ \text{K/MPa}\,,$$

and

$$0.005\ \text{cm}^3 < V < 0.15\ \text{cm}^3\,.$$

Equation (17) then gives

$$10\ \text{nuclei/(cm}^3\text{·s)} < J < 10^3\ \text{nuclei/(cm}^3\text{·s)}\,. \tag{19}$$

[A similar range is obtained if Eq. (12) is used with a characteristic waiting time of $\tau \simeq 1$ s.] The pool decompression method employed by Hord *et al.*[44] corresponded to a much lower nucleation rate—10^{-2} nuclei/(cm^3·s)—because of the large volume of superheated liquid ($\simeq$1000 cm^3).

Finally, floating droplet (i.e., the bubble column) methods have

$$0.03\ \text{K/s} < \dot{T} < 50\ \text{K/s}$$

and

$$10^{-7}\ \text{cm}^3 < V < 10^{-4}\ \text{cm}^3\,.$$

Equation (15) correspondingly gives

$$100\ \text{nuclei/(cm}^3\text{·s)} < J < 10^8\ \text{nuclei/(cm}^3\text{·s)}\,. \tag{20}$$

(The ranges of nucleation rate commensurate with the various experimental methods calculated above are very approximate values and were rounded off to the nearest order of magnitude.)

4.3. Pulse Heating Method

A pulsed current imposed on the platinum wire in this method rapidly heats the wire. This heating creates a thermal boundary layer, which propagates into the ambient liquid. The liquid in this boundary layer may eventually become superheated, after which the limit of superheat may ultimately be reached. The wire diameter will generally be large compared to the boundary layer thickness, so a plane approximation is valid. The intent is to estimate the number of bubbles that form a distance dx from the wire surface (of area A) in a liquid region of volume $A\cdot dx$.

The nucleation rate is the number of critical size nuclei that form in a unit volume and unit time. From Eq. (4) we have

$$J \simeq Ce^{-G}, \tag{21}$$

where $C \equiv \Gamma k_f N_0$ [Eq. (4)] and $G = \Delta\Phi^*/kT$. In the volume element $A\,dx$, the number of nuclei dn that form in the time dt is

$$dn = JA\,dx\,dt\,.$$

Then,

$$n = \int_0^{\tau}\int_0^{x} JA\,dx\,dt\,. \tag{22}$$

Since A is constant (the plane approximation)

$$n'' \equiv \frac{n}{A} = \int_0^{\tau}\int_0^{x} J\,dx\,dt\,, \tag{23}$$

where n'' is the number density (molecules per unit area) at the wire surface. Now following Skripov,[77] we recognize that $G = G(T)$ and $T = T(x,t)$. Expanding G in a Taylor series about T, and in turn T in a similar series about $x = 0$ and $t = \tau$, and retaining only the linear terms, yields

$$G \simeq G(T(x=0, t=\tau)) + G_T \frac{\partial T}{\partial t}(t-\tau) + G_T \frac{\partial T}{\partial x} \cdot x + \dots ,$$

where $\partial T/\partial t$ is the heating rate of the liquid and $\partial T/\partial x$ is the spatial temperature gradient. Combining the above equation with Eq. (21), substituting into Eq. (23), and integrating (assuming a constant heating rate) gives

$$J \simeq n'' G_T^2 \frac{\partial T}{\partial x} \cdot \frac{\partial T}{\partial t} . \tag{24}$$

In the thermal boundary layer (of thickness δ) the following approximations are made:

$$\frac{\partial T}{\partial x} \simeq \frac{T - T_0}{\delta} , \tag{25a}$$

where

$$\delta \simeq \sqrt{\alpha_l \tau} \tag{25b}$$

and

$$\frac{\partial T}{\partial t} \simeq \frac{T - T_0}{\tau} . \tag{25c}$$

Equation (24) therefore becomes

$$J \simeq n'' G_T^2 \frac{(T - T_0)^2}{\sqrt{\alpha_l}\, \tau^{3/2}} . \tag{26}$$

Equation (26) may be used to estimate J as follows. A typical order of magnitude of n'' for many organic liquids is 10^3 bubbles/cm^2 $< n'' <$ 10^4 bubbles/cm^2, while for water, $n'' \simeq 10^6$ bubbles/cm^2.[72] $T - T_0$ is directly inferred from the wire resistance (now $T \rightarrow T_k$ and T_0 is the bulk temperature—near room value). G_T can be estimated from the form of Eq. (4). We therefore arrive at the following estimates of the order of magnitude of nucleation rate commensurate with the pulse heating method. For

$$10^3 \text{ bubbles/cm}^2 < n'' < 10^6 \text{ bubbles/cm}^2 ,$$
$$3 \text{ K}^{-1} < G_T < 10 \text{ K}^{-1} ,$$
$$200 \text{ K} < T - T_0 < 300 \text{ K} ,$$
$$25\ \mu\text{s} < \tau < 1000\ \mu\text{s} ,$$
$$\sqrt{\alpha_l} \sim 10^{-2} \text{ cm/s}^{1/2} ,$$

Equation (26) yields a range of nucleation rates achievable with the pulse heating method of

$$10^{15} \text{ nuclei/cm}^3\text{·s} < J < 10^{22} \text{ nuclei/cm}^3\text{·s} . \tag{27}$$

A similar range (to within a few orders of magnitude) can be estimated by using Eq. (15) if it is assumed that critical size nuclei form in a superheated liquid layer at the heating surface, which has a thickness of the order of magnitude of the critical nucleus diameter.

The origin of this high range of rates compared to other methods is in the large wire heating rate ($\simeq 10^6$ K/s). The method of pulse heating a bismuth crystal[26,64,65] yielded a smaller effective nucleation rate—on the order of 10^7 nuclei/(cm^3·s)—primarily because the crystal was heated at a much smaller rate ($\simeq$10 K/s).

4.4. Summary

Table 3 summarizes the results of the previous two sections. Because of the (albeit weak) dependence of nucleation rate on temperature, the higher the effective nucleation rate produced by a particular method, the higher should be the measured limit of superheat. Differences in nucleation rates must be substantial, though, to yield measurable differences in limit of superheat: from Eq. (4) it may be shown that a three to four order of magnitude change in J will yield only a 1 K difference in calculated limit of superheat. Thus it may be expected that both variants of the capillary tube method (isobaric heating and isothermal decompression) will produce about the same value of limits of superheat. Floating droplet methods should yield limits of superheat a few degrees higher than capillary tube methods. The pulse heating method should unmistakably produce the highest superheat limits. Thus an internal consistency requirement of published data emerges from the effective nucleation rates produced by the various experimental methods,

$$T_4 > T_3 > T_2 \simeq T_1 , \tag{28}$$

where subscripts 1, 2, 3, and 4 refer to superheat limits measured by the isobaric heating and isothermal decompression variants of the capillary tube methods, the floating droplet method, and the pulse heating method, respectively. Data obtained from the various methods considered that did not conform to Eq. (28) were rejected.

Because of the simplifying approximations made in deriving Eqs. (15), (17), and (26), calculated nucleation rates corresponding to the various experimental methods are only rough estimates. It is unknown how inaccurate these estimates may be. The rather good agreement typically observed between measured and calculated superheat limits indicates that inaccuracies in precisely estimating J are insignificant. In fact, the above development is often ignored altogether when estimating the limit of superheat: $J = 1$ nucleus/(cm^3·s) is sometimes used to define the homogeneous nucleation limit (see Refs. 26, 53, 65, and 84, for example). The chief value of being more precise about the nucleation rate is in the insight such precision can give in explaining the definite differences in limits of superheat measured for a given liquid at a given pressure but using different methods.

TABLE 3. Approximate nucleation rates commensurate with various experimental methods

Method	J (cm^{-3}s^{-1})
1. Capillary tube	
Isobaric heating (Sec. 3.1.c)	1 to 10^3
Isothermal decompression (Sec. 3.2.c)	10^2 to 10^3
2. Floating droplets (Sec. 3.2)	10^2 to 10^8
3. Pulse heating (Sec. 3.1.b)	10^{15} to 10^{22}

5. Criteria for Inclusion of Data in Tables 4–6

5.1. Criteria

The following requirements had to be satisfied to warrant inclusion of published limits of superheat in the present compilation.

(1) The higher the effective nucleation rate commensurate with a given experimental method, the higher should be its limit of superheat. Equation (28) should therefore be satisfied. Limits of superheat obtained from the pulse heating method should be higher than values obtained from the floating droplet method at a given ambient pressure. Bubble column data should in turn (generally) be higher than superheat limits measured by capillary tube methods . The data listed in Tables 1 and 2 generally conformed to this rule.

(2) The limit of superheat must increase as ambient pressure increases when the nucleation rate varies by at most two or three orders of magnitude [see, for instance, Eqs. (5)–(7)].

(3) Enough information must be provided in the original reference, or the experimental method must be sufficiently established, that both the experimental uncertainty of reported superheat limits and an approximate nucleation rate commensurate with the experiment can be estimated.

(4) When one of the standard methods for measuring the limit of superheat was employed and the limit of superheat for a particular substance was reported only once by one investigating group, those data were included in Tables 4–6 (if the other criteria were also satisfied). This was done to provide a complete listing of the available data.

(5) When the limit of superheat for a particular substance was reported by a number of different investigating groups using various methods, an arithmetic average of the respective superheat limits at a given pressure, composition, and nucleation rate was taken to arrive at the values listed in Tables 4–6. The range for these values was less than 5 K. This average was rounded to the first decimal (except when the accuracy of measuring temperature was known to be more precise than this).[26,64,65] Given that the experimental uncertainty for all methods is of the order of a few degrees, all numbers listed in Tables 4–6 should not generally be considered more precise than this.

(6) It was not necessary that the reported data be theoretically verified in every case. Such verification of measurement with theory is the foundation of our understanding of homogeneous nucleation in superheated liquids. However, the paucity of relevant properties, the most important of which are bubble-point pressure and surface tension, precludes calculating the limit of superheat for all liquids. This problem is particularly severe for mixtures.[11] Those substances for which sufficient property data were available and which therefore were amenable to theoretical predictions [e.g., via Eqs. (5)–(7)] had superheat limits within a few degrees of measured values.

(7) Though the kinetic limit of superheat (T_k) must be less than the thermodynamic limit of superheat (T_t) at a given pressure [see Eq. (3)], to make practical use of this requirement, T_t must be calculated. Difficulties of the type discussed in Sec. 2 prevent such a calculation. Thus this requirement is only conceptual and cannot in practice be usefully applied.

5.2. Exceptions and Discrepancies

Most of the data in Tables 4–6 are internally consistent in that they satisfy the criteria stated in Sec. 5.1. A few of the data did not meet these criteria, yet are still included in the present compilation.

(1) The measurements of Sinha and co-workers,[17,63] Beams,[18] Apfel,[8] and Briggs[24,25] were most certainly influenced by gas bubble nucleation on the container walls. A comparison of some of their data with those obtained from other methods revealed, in some cases, substantial differences. In spite of these discrepancies, some of these data are included in the present compilation because they are the best available measurements of the extent of superheating (or dynamic stressing) of the particular liquids studied. Their inclusion in the final listing is meant to serve as a guide for future efforts to measure the limits of superheat or tensile strengths of the liquids in question.

(2) The limits of superheat of degassed methanol and ethanol reported in Ref. 54 showed apparently anomalous results compared to other published data. A substantial effect of degassing on the limit of superheat of methanol was noted (460.2 K for undegassed methanol versus 482 K for degassed methanol), while essentially no difference was observed for ethanol (472 versus 473 K). These two liquids are very close in structure so the origin of this difference is unknown. The degassed data reported in Ref. 54 were therefore not included in Table 4.

6. Data Extraction from Original Sources

The limits of superheat were reported in the original references in two ways: graphically and in the form of tabulated values.

Graphical presentation of data consisted of displaying the variation of superheat limit with either ambient pressure, composition, or waiting time. Figure quality had some bearing on the accuracy with which plotted data were reduced to tabular form for inclusion in the present compilation. In all cases, figures in the original sources were first enlarged. Each figure was then divided according to the indicated divisions on the coordinate axes and then subdivided into regions encompassing one or more of the plotted data. The coordinates of the data points were then obtained by scaling their locations in the respective subdivided regions in which they were located.

When data were presented in tabular form, they were extracted directly without modification. When the same data were presented in both tabular form and displayed graphically, they were extracted only from the table and the figures were not used.

The superheat limits listed in Tables 4–6 are presented

in the order of increasing composition, pressure (at each composition), and nucleation rate (at each pressure). Values are listed to the first decimal place.

All substances are listed in the first column in alphabetical order by chemical formula. Immediately beneath it, the name of the substance is given. Inorganic compounds are listed first, followed by organic compounds in the order of increasing carbon number.

Definition of Symbols for Figures 4–11 and Tables 4–6

T	Limit of superheat (K)
P	Pressure to which the limit of superheat corresponds (MPa)
J	Nucleation rate (nuclei/(cm^3·s)) commensurate with the experimental method used to measure the limit of superheat
x	Mole fraction of the second listed substance in the binary mixture
PH	Pulse heating method (Sec. 3.1.b)
BC1	Bubble column method: isobaric droplet heating (Sec. 3.2.b)
BC2	Bubble column method: isothermal decompression (Sec. 3.2.c)
CT1	Capillary tube: isobaric heating (Sec. 3.1.c)
CT2	Capillary tube: isothermal decompression (Sec. 3.1.c)
BUB	Bulb method (Sec. 3.1.d)

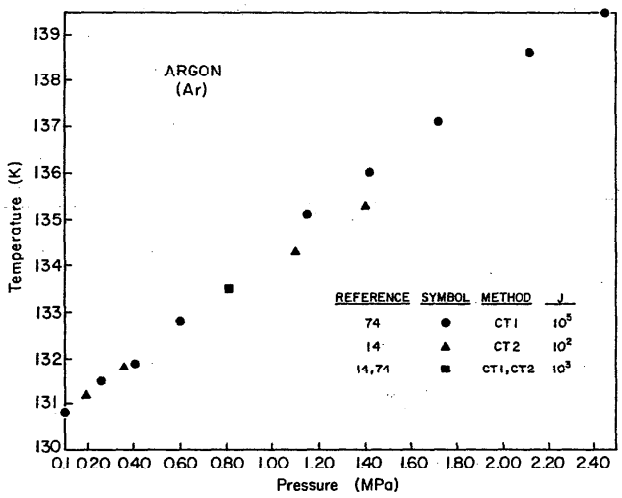

FIG. 4. Variation of limit of superheat of argon with pressure.

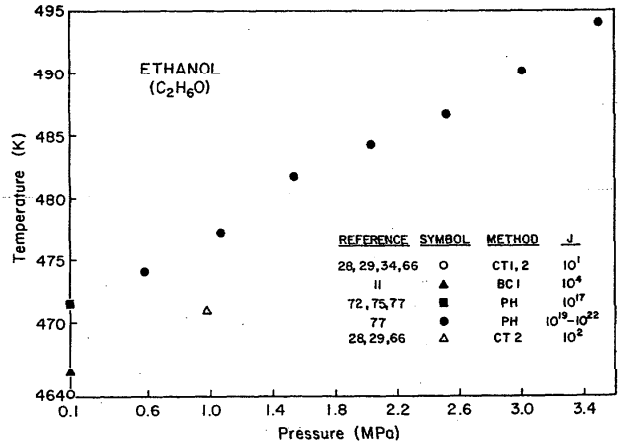

FIG. 6. Variation of limit of superheat of ethanol with pressure.

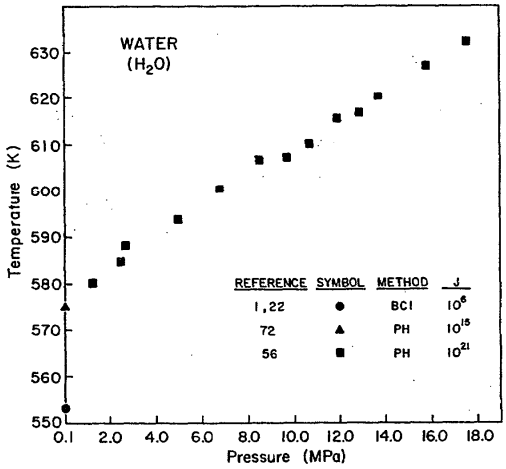

FIG. 5. Variation of limit of superheat of water with pressure.

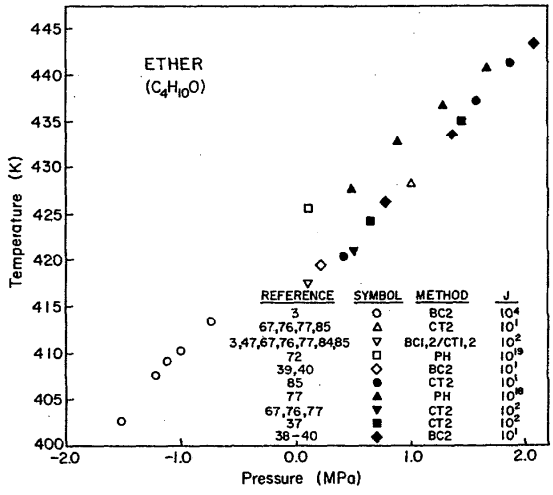

FIG. 7. Variation of limit of superheat and tensile strengths (negative pressures) of ether with pressure.

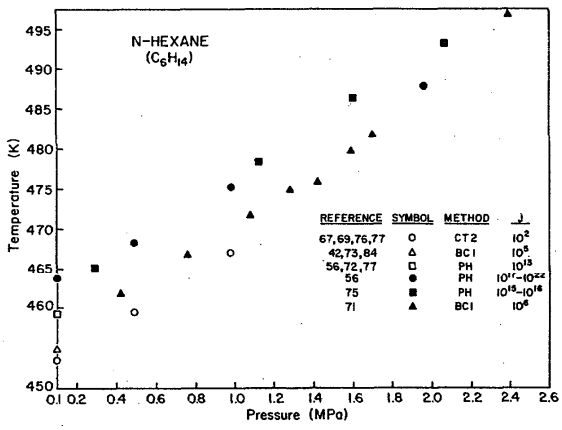

FIG. 8. Variation of limit of superheat of *n*-hexane with pressure.

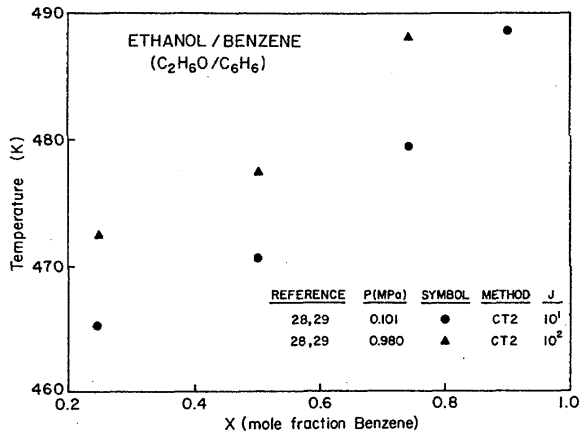

FIG. 10. Variation of limit of superheat of ethanol/benzene mixtures with mole fraction benzene at 0.101 and 0.98 MPa.

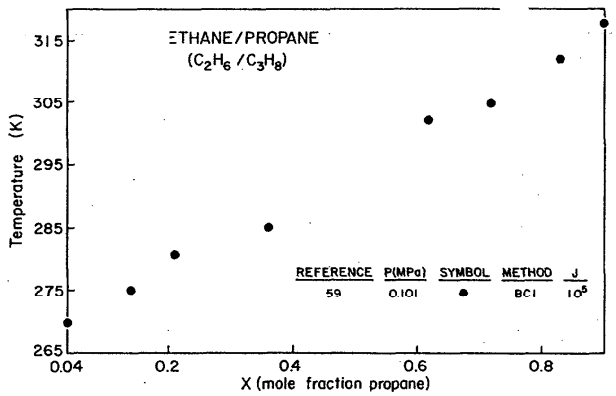

FIG. 9. Variation of limit of superheat of ethane/*n*-propane mixtures with mole fraction propane at 0.101 MPa.

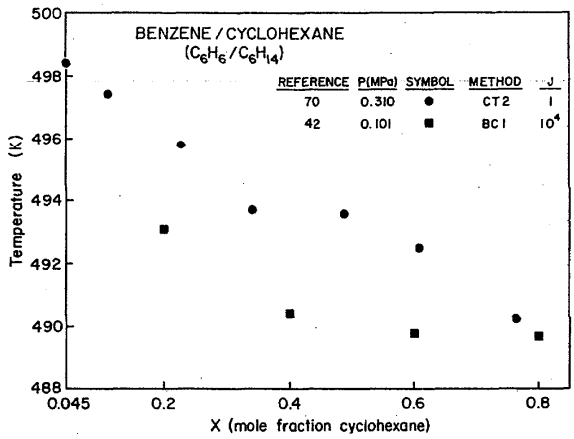

FIG. 11. Variation of limit of superheat of benzene/cyclohexane mixtures with mole fraction cyclohexane at 0.101 and 0.310 MPa.

Table 4: Limits of superheat of pure liquids

Substance	P [MPa]	T [K]	J [nuclei/(cm^3•s)]	Method	Reference
1. Ar	-1.220	85.0	1E+02	CT2	18
Argon	0.101	130.8	1E+02	CT1	74
	0.190	131.2	1E+02	CT2	14
	0.260	131.5	1E+05	CT1	74
	0.360	131.8	1E+01	CT2	14
	0.410	131.9	1E+05	CT1	74
	0.600	132.8	1E+05	CT1	74
	0.810	133.5	1E+03	CT1,2	74
	1.100	134.3	1E+01	CT2	14
	1.150	135.1	1E+05	CT1	74
	1.400	135.3	1E+01	CT2	14
	1.420	136.0	1E+05	CT1	74
	1.720	137.1	1E+05	CT1	74
	2.140	138.6	1E+05	CT1	74
	2.450	139.5	1E+05	CT1	74
	2.710	141.3	1E+05	CT1	74
2. H_2	.076	27.8	1E-02	CT2	44
Hydrogen	.149	27.9	1E-02	CT2	44
	.381	29.4	1E-02	CT2	44
	.751	30.6	1E-02	CT2	44
	.834	30.8	1E-02	CT2	44
3. H_2O	-27.700	283.2	1E+03	CT2	24,25
Water	0.101	553.0	1E+06	BC1	1,22
	0.101	575.2	1E+15	PH	72
	1.293	580.4	1E+21	PH	56
	2.519	584.9	1E+21	PH	56
	2.710	588.3	1E+21	PH	56
	5.000	593.6	1E+21	PH	56
	6.808	600.4	1E+21	PH	56
	8.500	606.5	1E+21	PH	56
	9.731	607.2	1E+21	PH	56
	10.746	610.3	1E+21	PH	56
	11.978	615.6	1E+21	PH	56
	12.873	616.7	1E+21	PH	56
	13.731	620.2	1E+21	PH	56
	15.789	627.0	1E+21	PH	56
	17.556	632.3	1E+21	PH	56
	20.113	642.2	1E+21	PH	56
4. He I	0.012	4.05	1E+07	PH	64
Helium I	0.017	4.12	1E+07	PH	64
	0.037	4.22	1E+07	PH	65
	0.054	4.31	1E+07	PH	65
	0.066	4.37	1E+07	PH	65
	0.081	4.45	1E+07	PH	65
	0.100	4.55	1E+07	PH	65
	0.112	4.62	1E+07	PH	64
	0.129	4.70	1E+07	PH	64
	0.143	4.76	1E+07	PH	64

Table 4: Limits of superheat of pure liquids — Continued

Substance	P [MPa]	T [K]	J [nuclei/(cm^3•s)]	Method	Reference
5. He II Helium II	-0.06	2.09	1E+05	CT2	50
6. Kr Krypton	0.400	182.5	1E+05	CT1	74
	0.820	184.3	1E+05	CT1	74
	1.200	187.0	1E+05	CT1	74
	1.410	187.6	1E+05	CT1	74
	1.630	189.1	1E+05	CT1	74
	1.900	189.9	1E+05	CT1	74
	2.200	192.1	1E+05	CT1	74
	2.430	192.9	1E+05	CT1	74
	2.800	194.8	1E+05	CT1	74
	3.140	196.6	1E+05	CT1	74
	3.460	198.0	1E+05	CT1	74
	3.800	199.4	1E+05	CT1	74
7. N_2 Nitrogen	-1.010	75.0	1E+02	CT2	18
	0.101	110.0	1E+00	CT1	53
	0.410	111.4	1E+05	CT1	15
	0.520	112.0	1E+05	CT1	15
	0.610	112.1	1E+05	CT1	15
	0.700	112.7	1E+05	CT1	15
	0.820	113.2	1E+05	CT1	15
	0.940	113.8	1E+05	CT1	15
	1.060	114.2	1E+05	CT1	15
	1.210	114.8	1E+05	CT1	15
	1.240	115.2	1E+05	CT1	15
	1.330	115.5	1E+05	CT1	15
	1.360	115.6	1E+05	CT1	15
	1.460	116.2	1E+05	CT1	15
	1.590	116.8	1E+05	CT1	15
	1.620	117.0	1E+05	CT1	15
	1.730	117.6	1E+05	CT1	15
	1.770	117.7	1E+05	CT1	15
	1.870	118.3	1E+05	CT1	15
	1.920	118.4	1E+05	CT1	15
	2.070	119.1	1E+05	CT1	15
8. N_2O_3 Nitrogen-tetroxide	0.154	395.6	1E+02	CT2	83
	0.554	396.2	1E+02	CT2	83
	0.980	398.2	1E+01	CT2	83
	2.000	401.5	1E+01	CT2	83
	3.040	405.2	1E+01	CT2	83
	3.920	408.1	1E+01	CT2	83
	4.500	410.2	1E+01	CT2	83
	5.000	412.5	1E+01	CT2	83
	5.500	414.5	1E+01	CT2	83
	6.000	416.4	1E+01	CT2	83

Table 4: Limits of superheat of pure liquids — Continued

Substance	P [MPa]	T [K]	J [nuclei/(cm^3•s)]	Method	Reference
9. O_2 Oxygen	-1.520	75.0	1E+02	CT2	18
	0.101	134.1	1E+00	CT1	53
	0.400	135.4	1E+05	CT1	15
	0.500	136.2	1E+05	CT1	15,30
	0.680	136.5	1E+05	CT1	15,30
	0.920	137.4	1E+05	CT1	30
	1.060	137.5	1E+05	CT1	15,30
	1.180	138.3	1E+05	CT1	15,30
	1.350	138.9	1E+05	CT1	15,30
	1.480	139.3	1E+05	CT1	15,30
	1.740	140.7	1E+05	CT1	15,30
	2.030	141.9	1E+05	CT1	15,30
	2.260	142.8	1E+05	CT1	15,30
	2.500	143.6	1E+05	CT1	15,30
	2.700	144.5	1E+05	CT1	15,30
	2.970	145.9	1E+05	CT1	15,30
10. SO_2 Sulphur-dioxide	0.101	323.2	1E+02	CT1	47
11. Xe Xenon	0.500	254.1	1E+05	CT1	74
	0.830	256.3	1E+05	CT1	74
	1.070	257.2	1E+05	CT1	74
	1.260	258.2	1E+05	CT1	74
	1.470	259.6	1E+05	CT1	74
	1.550	260.3	1E+05	CT1	74
	1.680	261.0	1E+05	CT1	74
	1.750	261.6	1E+05	CT1	74
	1.860	261.9	1E+05	CT1	74
	1.970	262.8	1E+05	CT1	74
	2.070	263.4	1E+05	CT1	74
	2.170	263.8	1E+05	CT1	74
	2.370	265.2	1E+05	CT1	74
11. Xe Xenon (Contd.)	2.480	266.1	1E+05	CT1	74
	2.630	266.9	1E+05	CT1	74
	2.750	267.5	1E+05	CT1	74
	2.850	267.8	1E+05	CT1	74
	2.970	269.1	1E+05	CT1	74
	3.050	269.7	1E+05	CT1	74
	3.130	270.0	1E+05	CT1	74
	3.450	272.0	1E+05	CT1	74
	3.630	273.0	1E+05	CT1	74
12. $ClCHF_2$ Chloro-difluoro-methane	0.101	327.8	1E+04	BC1	52
	0.236	328.2	1E+04	BC1	52
	0.280	329.4	1E+04	BC1	52
	0.510	330.8	1E+04	BC1	52
	0.560	331.5	1E+04	BC1	52
	0.710	332.4	1E+04	BC1	52

Table 4: Limits of superheat of pure liquids — Continued

Substance	P [MPa]	T [K]	J [nuclei/(cm^3•s)]	Method	Reference
12. $ClCHF_2$ Chloro-difluoro-methane (Cont.)	0.810	332.9	1E+04	BC1	52
	0.910	334.2	1E+04	BC1	52
13. $C_2Cl_2H_2F_2$ Dichloro-difluoro-ethane	0.221	342.5	1E+06	BC2	51
	0.427	344.3	1E+06	BC2	51
	0.462	344.7	1E+06	BC2	51
	0.655	346.6	1E+06	BC2	51
	0.896	348.8	1E+06	BC2	51
	0.931	349.0	1E+06	BC2	51
	1.227	351.7	1E+06	BC2	51
	1.489	354.4	1E+06	BC2	51
	1.917	358.8	1E+06	BC2	51
	2.399	363.7	1E+06	BC2	51
	2.910	369.0	1E+06	BC2	51
	3.289	373.0	1E+06	BC2	51
	3.323	373.4	1E+06	BC2	51
	3.585	376.2	1E+06	BC2	51
	3.634	376.9	1E+06	BC2	51
14. CCl_4 Carbon tetra-chloride	-27.600	268.2	1E+03	CT2	25
15. $CHCl_3$ Chloroform	-31.700	258.2	1E+03	CT2	25
	0.101	466.2	1E+02	CT1	47
16. CH_2Cl_2 Methylene-chloride	0.101	394.8	1E+01	BUB	17
17. CH_3Cl Chloro-methane	0.101	366.2	1E+05	BC1	59
18. CH_4 Methane	0.400	167.6	1E+05	CT1	15
	0.620	168.3	1E+05	CT1	15
	0.820	169.3	1E+05	CT1	15
	1.030	170.5	1E+05	CT1	15
	1.230	171.4	1E+05	CT1	15
	1.430	172.1	1E+05	CT1	15
	1.630	173.1	1E+05	CT1	15
	1.830	174.0	1E+05	CT1	15
	2.030	175.2	1E+05	CT1	15
	2.220	176.4	1E+05	CT1	15
	2.430	177.6	1E+05	CT1	15
	2.630	178.6	1E+05	CT1	15
	2.820	180.0	1E+05	CT1	15

Table 4: Limits of superheat of pure liquids — Continued

Substance	P [MPa]	T [K]	J [nuclei/(cm^3·s)]	Method	Reference
9. CH_4O Methanol	0.101	458.4	1E+01	CT1,2	34,66
	0.101	461.2	1E+05	BC1	11,54
	0.101	466.2	1E+18	PH	72,77
	0.600	469.2	1E+19	PH	77
	1.050	471.2	1E+20	PH	77
	2.030	476.7	1E+16	PH	77
	2.030	478.2	1E+20	PH	77
	3.000	482.2	1E+21	PH	77
	4.000	488.7	1E+22	PH	77
	4.980	494.7	1E+22	PH	77
	5.970	501.2	1E+23	PH	77
	6.960	507.7	1E+23	PH	77
20. C_2H_3Cl Chloroethane	0.101	374.1	1E+05	BC1	59
21. C_2H_3F Fluoroethene	0.101	290.1	1E+05	BC1	59
22. C_2H_3N Acetonitrile	0.101	497.0	1E+06	BC1	55
23. $C_2H_4F_2$ 1,1-Difluoro-ethane	0.101	343.6	1E+05	BC1	59
24. $C_2H_4O_2$	-28.800	292.7	1E+03	CT2	25
Acetic acid	0.101	526.2	1E+06	BC1	55
25. $C_2H_4O_2$ Methyl-formate	0.101	423.2	1E+01	BUB	17
26. C_2H_5Br Ethylbromide	0.101	422.2	1E+01	BUB	63
27. C_2H_5Cl Ethylchloride	0.101	399.2	1E+01	CT1	85
28. C_2H_6 Ethane	0.101	269.2	1E+05	BC1	59
29. C_2H_6O	0.101	464.1	1E+01	CT1,2	28,29,34,66
Ethanol	0.101	466.0	1E+04	BC1	11
	0.101	471.5	1E+17	PH	72,75,77
	0.580	474.2	1E+19	PH	77
	0.980	471.0	1E+02	CT2	28,29,66
	1.070	477.2	1E+20	PH	77
	1.540	481.7	1E+20	PH	77
	2.030	484.2	1E+21	PH	77
	2.520	486.7	1E+21	PH	77
	3.010	490.2	1E+21	PH	77
	3.500	494.2	1E+22	PH	77

Table 4: Limits of superheat of pure liquids — Continued

Substance	P [MPa]	T [K]	J [nuclei/(cm^3·s)]	Method	Reference
30. C_3H_3N Acrylonitrile	0.101	489.0	1E+05	BC1	55
31. C_3H_4 Propadiene	0.101	346.2	1E+05	BC1	59
32. C_3H_4 Propyne	0.101	356.8	1E+05	BC1	59
33. C_3H_6 Cyclopropane	0.101	350.7	1E+05	BC1	59
34. C_3H_6 Propene	0.101	325.6	1E+05	BC1	59
35. C_3H_6O Acetone	0.101	454.5	1E+01	CT2	29
	0.101	456.4	1E+02	CT2	28,66
	0.101	458.7	1E+13	PH	72
	0.101	462.7	1E+18	PH	72
	0.980	462.6	1E+01	CT2	29,66
36. $C_3H_6O_2$ Ethylformate	0.101	428.5	1E+01	BUB	17
37. $C_3H_6O_2$ Methylacetate	0.101	416.6	1E+01	BUB	17
38. C_3H_8 N-Propane	0.101	326.4	1E+06	BC1	59,61
	0.302	332.8	1E+04	BC1	52
	0.491	336.8	1E+04	BC1	52
	0.715	339.1	1E+04	BC1	52
	0.907	343.2	1E+04	BC1	52
39. C_3H_8O N-Propanol	0.101	487.4	1E+04	BC1	11
	0.101	493.0	1E+15	PH	72
	0.101	495.7	1E+18	PH	72
40. C_3H_8O Isopropanol	0.101	473.0	1E+06	BC1	55
41. C_4H_6 1,3-Butadene	0.101	377.3	1E+05	BC1	59
42. C_4H_8 1-Butene	0.101	371.0	1E+05	BC1	59
43. C_4H_8 Butylene	0.101	510.2	1E+16	PH	75

Table 4: Limits of superheat of pure liquids — Continued

Substance	P [MPa]	T [K]	J [nuclei/(cm^3•s)]	Method	Reference
44. C_4H_8 Cis-2-Butene	0.101	385.4	1E+05	BC1	59
45. C_4H_8 Trans-2-Butene	0.101	379.7	1E+05	BC1	59
46. C_4H_8 2-Methylpropene	0.101	369.6	1E+05	BC1	59
47. C_4H_{10} N-Butane	0.101	377.6	1E+05	BC1	33,59,61,62
48. C_4H_{10} 2-Methylpropane	0.101	361.0	1E+05	BC1	59
49. $C_4H_{10}O$ N-Butanol	0.101	509.6	1E+02	CT2	28,29,66
	0.101	511.9	1E+04	BC1	11
	0.101	513.2	1E+13	PH	72
	0.101	516.2	1E+16	PH	72
	0.101	518.2	1E+18	PH	72
	0.980	519.4	1E+02	CT2	29,66
50. $C_4H_{10}O$ Ether	-1.75	293.	1E+02	CT2	8
	-1.520	402.7	1E+04	BC2	3
	-1.220	407.6	1E+04	BC2	3
	-1.120	409.2	1E+04	BC2	3
	-1.000	410.2	1E+04	BC2	3
	-0.740	413.4	1E+04	BC2	3
	0.101	417.5	1E+02	BC1,2/CT1,2	3,47,67,76, 77,84,85
	0.101	425.7	1E+19	PH	72
	0.211	419.4	1E+01	BC2	39,40
	0.415	420.3	1E+01	CT2	85
	0.480	427.7	1E+18	PH	77
	0.500	421.1	1E+02	CT2	67,76,77
	0.641	424.3	1E+02	CT2	37
	0.777	426.3	1E+01	BC2	38-40
	0.880	432.7	1E+18	PH	77
	1.000	428.4	1E+01	CT2	67,76,77,85
	1.280	436.7	1E+01	PH	77
	1.366	433.6	1E+01	BC2	38-40
	1.442	435.1	1E+02	CT2	37
	1.575	437.2	1E+01	CT2	85
	1.660	440.7	1E+19	PH	77
	1.865	441.2	1E+01	CT2	85
	2.089	443.3	1E+01	BC2	38-40
	2.450	450.7	1E+21	PH	77
	2.850	455.7	1E+20	PH	77
51. $C_4H_{10}O$ Isobutanol	0.101	437.2	1E+01	BUB	17

Table 4: Limits of superheat of pure liquids — Continued

Substance	P [MPa]	T [K]	J [nuclei/(cm^3•s)]	Method	Reference
52. $C_4H_{11}N$ Diethylamine	0.101	408.5	1E+01	BUB	17
53. C_5F_{12} Perfluoro-	0.101	381.5	1E+06	BC1	36
pentane	0.300	385.4	1E+06	BC1	36
	0.500	388.7	1E+06	BC1	36
	0.700	392.2	1E+06	BC1	36
	0.890	396.4	1E+06	BC1	36
	1.090	399.0	1E+06	BC1	36
	1.280	403.1	1E+06	BC1	36
	1.480	407.4	1E+06	BC1	36
54. C_5H_8 Cyclopentene	0.101	451.4	1E+06	BC1	33
55. C_5H_{10} Cyclopentane	0.101	455.1	1E+06	BC1	33,84
56. C_5H_{10} 1-Pentene	0.101	417.2	1E+06	BC1	33
57. C_5H_{12} 2,2-Dimethyl- propane	0.101	386.1	1E+06	BC1	33
58. C_5H_{12}	0.101	409.2	1E+01	CT2	85
Isopentane	0.101	411.7	1E+07	BC1	73,84
59. C_5H_{12}	0.101	418.8	1E+04	BC1/CT2	22,27,42,45,
N-Pentane					61,67,68,71,
					73,76-78,84
	0.101	426.2	1E+18	PH	72
	0.490	423.7	1E+02	CT2	66-68,76,77
	0.880	429.1	1E+02	CT2	66-68,76,77
	1.280	435.3	1E+02	CT2	66-68,76,77
	2.600	451.2	1E+06	BC1	78
60. $C_5H_{12}O$ N-Pentanol	0.101	532.2	1E+17	PH	77
61. C_6F_6 Hexafluoro-	0.101	464.8	1E+01	CT2	77
benzene	0.101	467.9	1E+06	BC1	35
	0.500	469.9	1E+02	CT2	77
	0.570	474.1	1E+06	BC1	35
	1.000	477.1	1E+02	CT2	77
	1.050	480.4	1E+06	BC1	35
	1.540	486.0	1E+06	BC1	35
	2.030	494.2	1E+06	BC1	35

Table 4: Limits of superheat of pure liquids — Continued

Substance	P [MPa]	T [K]	J [nuclei/(cm^3•s)]	Method	Reference
62. C_6F_{14} Perfluoro-hexane	0.101	409.8	1E+06	BC1	36
	0.300	414.4	1E+06	BC1	36
	0.500	418.5	1E+06	BC1	36
	0.700	422.3	1E+06	BC1	36
	0.880	425.6	1E+06	BC1	36
	1.050	430.3	1E+06	BC1	36
	1.240	434.6	1E+06	BC1	36
63. C_6H_5Br Bromobenzene	0.101	534.2	1E+02	CT1	47
64. C_6H_5Cl Chlorobenzene	0.101	523.2	1E+02	CT1	47
65. C_6H_6 Benzene	-15.000	291.2	1E+03	CT2	25
	0.101	498.9	1E+02	CT2/BC1	28,29,42, 67,76,77
	0.101	510.2	1E+18	PH	72
	0.490	502.2	1E+02	CT2	67,76,77
	0.580	514.2	1E+19	PH	56
	0.980	509.2	1E+02	CT2	28,29,67,76
	1.070	516.7	1E+18	PH	56
	1.470	513.8	1E+02	CT2	67,76,77
	1.540	520.7	1E+19	PH	56
	2.030	525.7	1E+19	PH	56
	2.520	532.2	1E+20	PH	56
	3.010	537.7	1E+17	PH	77
	3.500	544.7	1E+18	PH	56
66. C_6H_7N Aniline	-30.000	272.2	1E+03	CT2	25
	0.101	535.2	1E+02	CT1	47
67. C_6H_{12} Cyclohexane	0.101	490.8	1E+06	CT2/BC1	33,35,42,84
	0.300	493.1	1E+02	CT2	66,70
	0.420	495.2	1E+06	BC1	35
	0.720	499.7	1E+06	BC1	35
	0.950	501.7	1E+06	BC1	35
	0.980	502.1	1E+02	CT2	66
	1.110	504.2	1E+06	BC1	35
	1.350	506.2	1E+06	BC1	35
	1.700	512.2	1E+06	BC1	35
	2.160	518.2	1E+06	BC1	35
	2.370	519.2	1E+06	BC1	35
	2.550	523.2	1E+06	BC1	35
68. C_6H_{12} 1-Hexyne	0.101	465.2	1E+06	BC1	33
69. C_6H_{12} Methylcyclo-pentane	0.101	476.1	1E+06	BC1	33

Table 4: Limits of superheat of pure liquids — Continued

Substance	P [MPa]	T [K]	J [nuclei/(cm^3·s)]	Method	Reference
70. C_6H_{14} 2,3-Dimethyl-butane	0.101	446.4	1E+06	BC1	33
71. C_6H_{14} N-Hexane	0.101	453.5	1E+02	CT2	67,69,76,77
	0.101	454.9	1E+05	BC1	42,73,84
	0.101	459.2	1E+13	PH	56,72,77
	0.101	463.7	1E+20	PH	56
	0.290	465.2	1E+15	PH	75
	0.420	461.7	1E+06	BC1	71
	0.490	459.3	1E+02	CT2	67,69,76,77
	0.490	468.2	1E+22	PH	56
	0.760	466.7	1E+06	BC1	71
	0.980	467.0	1E+02	CT2	67,69,76,77
	0.980	475.2	1E+23	PH	56
	1.080	471.7	1E+06	BC1	71
	1.120	478.2	1E+15	PH	75
	1.280	474.7	1E+06	BC1	71
	1.420	475.7	1E+06	BC1	71
	1.590	479.7	1E+06	BC1	71
	1.600	486.2	1E+16	PH	75
	1.720	481.7	1E+06	BC1	71
	1.960	487.7	1E+17	PH	56
	2.060	493.2	1E+16	PH	75
	2.390	496.7	1E+06	BC1	71
	2.570	501.2	1E+16	PH	75
72. $C_6H_{14}O$ N-Hexanol	0.101	551.7	1E+04	BC1	11
73. C_7F_8 Octafluoro-	0.101	485.3	1E+01	CT3	66
toluene	0.490	489.7	1E+01	CT3	66
	0.980	499.8	1E+01	CT3	66
74. C_7F_{16} Perfluoro-	0.101	434.8	1E+06	BC1	36
heptane	0.230	436.9	1E+06	BC1	36
	0.400	440.5	1E+06	BC1	36
	0.570	444.4	1E+06	BC1	36
	0.770	448.3	1E+06	BC1	36
	0.920	452.7	1E+06	BC1	36
	1.070	456.1	1E+06	BC1	36
	1.150	459.0	1E+06	BC1	36
	1.280	461.3	1E+06	BC1	36
75. C_7H_8 Toluene	0.101	526.7	1E+02	CT3	66
76. C_7H_{14} Methylcyclo-hexane	0.101	510.4	1E+06	BC1	33

Table 4: Limits of superheat of pure liquids — Continued

Substance	P [MPa]	T [K]	J [nuclei/(cm^3•s)]	Method	Reference
77. C_7H_{16} N-Heptane	0.101	486.9	1E+06	BC1	12,33,55,71
	0.101	493.7	1E+18	PH	72
	0.294	489.2	1E+06	BC1	71
	0.392	490.7	1E+06	BC1	71
	0.490	493.7	1E+06	BC1	71
	0.589	494.2	1E+06	BC1	71
	0.736	498.7	1E+06	BC1	71
	0.952	500.7	1E+06	BC1	71
	1.275	505.2	1E+06	BC1	71
	1.373	509.7	1E+06	BC1	71
	1.570	512.7	1E+06	BC1	71
	1.736	515.2	1E+06	BC1	71
	1.805	516.7	1E+06	BC1	71
	2.001	519.7	1E+06	BC1	71
78. $C_7H_{16}O$ N-Heptanol	0.101	566.3	1E+04	BC1	11
79. C_8F_{18} Perfluoro-octane	0.101	457.0	1E+06	BC1	36
	0.300	461.1	1E+06	BC1	36
	0.500	467.1	1E+06	BC1	36
	0.700	471.2	1E+06	BC1	36
	0.890	476.9	1E+06	BC1	36
	1.090	482.8	1E+06	BC1	36
	1.190	484.1	1E+06	BC1	36
80. C_8H_{10} Cyclo-octane	0.101	560.7	1E+06	BC1	33
81. C_8H_{10} 2,3-dimethyl-benzene	0.101	508.2	1E+02	CT1	47
82. C_8H_{16} 1-Octene	0.101	510.3	1E+06	BC1	33
83. C_8H_{18} N-Octane	0.101	513.8	1E+06	BC1	13,33,61
	0.377	519.3	1E+04	BC1	13
	0.653	525.2	1E+04	BC1	13
	0.929	528.6	1E+04	BC1	13
	1.204	532.4	1E+04	BC1	13
84. C_8H_{18} 2,2,4-Trimethyl-pentane	0.101	488.5	1E+06	BC1	33
85. $C_8H_{18}O$ N-Octanol	0.101	586.0	1E+04	BC1	11

Table 4: Limits of superheat of pure liquids — Continued

Substance	P [MPa]	T [K]	J [nuclei/(cm^3•s)]	Method	Reference
86. C_9F_{20} Perfluoro-nonane	0.101	478.5	1E+06	BC1	36
	0.300	484.4	1E+06	BC1	36
	0.500	489.3	1E+06	BC1	36
	0.700	493.3	1E+06	BC1	36
	0.890	499.7	1E+06	BC1	36
	1.090	505.7	1E+06	BC1	36
87. C_9H_{20} N-Nonane	0.101	538.5	1E+06	BC1	33
88. $C_{10}F_{22}$ Perfluoro-decane	0.101	497.1	1E+06	BC1	36
	0.300	503.2	1E+06	BC1	36
	0.500	508.6	1E+06	BC1	36
	0.700	515.6	1E+06	BC1	36
	0.890	521.2	1E+06	BC1	36
	1.090	527.7	1E+06	BC1	36
89. $C_{10}H_{22}$ N-Decane	0.101	558.3	1E+06	BC1	33
90. $C_{12}H_{10}O$ Diphenyl-ether	0.101	703.2	1E+17	PH	72
	0.101	708.7	1E+19	PH	72

Table 5: Limits of superheat of binary mixtures

Substance	X	P [MPa]	T [K]	J [nuclei/(cm^3•s)]	Method	Reference
1. $CHCl_3/C_5H_{12}$ Chloroform/ N-pentane	0.270	0.101	429.6	1E+05	BC1	27
2. $CH_4O/C_2H_4O_2$ Methanol/ Acetic acid	0.500	0.101	481.0	1E+04	BC1	54
3. $CO_2/ClCHF_2$ Carbon Dioxide(Gas)/ Freon 22	0.820	0.095	309.0	1E+04	BC1	52
	0.820	0.350	311.7	1E+04	BC1	52
	0.820	0.510	312.9	1E+04	BC1	52
	0.820	0.610	313.6	1E+04	BC1	52
	0.820	0.710	314.1	1E+04	BC1	52
	0.820	0.810	315.0	1E+04	BC1	52
	0.820	0.910	315.5	1E+04	BC1	52
	0.820	1.020	316.2	1E+04	BC1	52
	0.870	0.110	314.3	1E+04	BC1	52
	0.870	0.250	315.2	1E+04	BC1	52
	0.870	0.350	316.6	1E+04	BC1	52
	0.870	0.460	317.1	1E+04	BC1	52
	0.870	0.530	317.5	1E+04	BC1	52
	0.870	0.650	318.2	1E+04	BC1	52
	0.870	0.770	319.1	1E+04	BC1	52
	0.870	0.850	319.4	1E+04	BC1	52
	0.870	0.910	319.7	1E+04	BC1	52
	0.870	0.990	320.1	1E+04	BC1	52
	0.910	0.095	319.0	1E+04	BC1	52
	0.910	0.193	319.8	1E+04	BC1	52
	0.910	0.460	321.2	1E+04	BC1	52
	0.910	0.490	321.8	1E+04	BC1	52
	0.910	0.610	322.5	1E+04	BC1	52
	0.910	0.740	323.5	1E+04	BC1	52
	0.910	0.810	324.1	1E+04	BC1	52
	0.910	0.850	324.5	1E+04	BC1	52
	0.910	0.910	324.7	1E+04	BC1	52
	0.910	0.960	325.4	1E+04	BC1	52
	0.910	1.010	326.0	1E+04	BC1	52
	0.970	0.095	323.5	1E+04	BC1	52
	0.970	0.148	323.9	1E+04	BC1	52
	0.970	0.182	324.4	1E+04	BC1	52
	0.970	0.230	324.9	1E+04	BC1	52
	0.970	0.280	325.2	1E+04	BC1	52
	0.970	0.370	325.6	1E+04	BC1	52
	0.970	0.400	325.9	1E+04	BC1	52
	0.970	0.560	327.4	1E+04	BC1	52
	0.970	0.740	329.2	1E+04	BC1	52
	0.970	0.810	329.5	1E+04	BC1	52
	0.970	0.910	330.1	1E+04	BC1	52
	0.970	1.010	330.8	1E+04	BC1	52

Table 5: Limits of superheat of binary mixtures—Continued

Substance	X	P [MPa]	T [K]	J [nuclei/(cm^3•s)]	Method	Reference
4. CO_2/C_3H_8 Carbon Dioxide(Gas)/ N-Propane	0.700	0.106	307.1	1E+04	BC1	52
	0.700	0.302	309.0	1E+04	BC1	52
	0.700	0.410	310.2	1E+04	BC1	52
	0.700	0.509	312.0	1E+04	BC1	52
	0.700	0.715	314.8	1E+04	BC1	52
	0.700	0.810	316.2	1E+04	BC1	52
	0.700	1.014	318.3	1E+04	BC1	52
	0.780	0.106	313.6	1E+04	BC1	52
	0.780	0.302	315.0	1E+04	BC1	52
	0.780	0.410	316.6	1E+04	BC1	52
	0.780	0.509	318.2	1E+04	BC1	52
	0.780	0.715	320.1	1E+04	BC1	52
	0.780	0.810	320.8	1E+04	BC1	52
	0.780	0.912	321.8	1E+04	BC1	52
	0.780	1.014	324.3	1E+04	BC1	52
	0.850	0.106	319.7	1E+04	BC1	52
	0.850	0.302	321.5	1E+04	BC1	52
	0.850	0.410	322.2	1E+04	BC1	52
	0.850	0.715	325.5	1E+04	BC1	52
	0.850	0.810	327.5	1E+04	BC1	52
	0.850	1.014	329.7	1E+04	BC1	52
	0.910	0.106	324.3	1E+04	BC1	52
	0.910	0.208	324.5	1E+04	BC1	52
	0.910	0.302	325.9	1E+04	BC1	52
	0.910	0.410	326.6	1E+04	BC1	52
	0.910	0.509	327.5	1E+04	BC1	52
	0.910	0.715	330.5	1E+04	BC1	52
	0.910	0.810	332.0	1E+04	BC1	52
	0.910	0.912	332.8	1E+04	BC1	52
	0.910	1.014	334.1	1E+04	BC1	52
5. CO_2/C_4H_{10} Carbon Dioxide(Gas)/ Isobutane	0.670	0.101	314.3	1E+04	BC1	52
	0.670	0.208	315.0	1E+04	BC1	52
	0.670	0.301	315.8	1E+04	BC1	52
	0.670	0.407	316.6	1E+04	BC1	52
	0.670	0.611	319.3	1E+04	BC1	52
	0.670	0.712	320.4	1E+04	BC1	52
	0.670	0.813	321.7	1E+04	BC1	52
	0.670	1.070	326.3	1E+04	BC1	52
	0.740	0.208	326.3	1E+04	BC1	52
	0.740	0.301	327.1	1E+04	BC1	52
	0.740	0.407	327.4	1E+04	BC1	52
	0.740	0.514	329.4	1E+04	BC1	52
	0.740	0.611	330.3	1E+04	BC1	52
	0.740	0.718	331.7	1E+04	BC1	52
	0.740	0.818	333.7	1E+04	BC1	52
	0.740	0.910	334.6	1E+04	BC1	52
	0.740	1.020	335.9	1E+04	BC1	52
	0.740	1.070	336.9	1E+04	BC1	52
	0.740	1.120	337.3	1E+04	BC1	52

Table 5: Limits of superheat of binary mixtures—Continued

Substance	X	P [MPa]	T [K]	J [nuclei/(cm^3•s)]	Method	Reference
5. CO_2/C_4H_{10}	0.800	0.101	330.3	1E+04	BC1	52
Carbon	0.800	0.208	332.5	1E+04	BC1	52
Dioxide(Gas)/	0.80	0.329	333.7	1E+04	BC1	52
Isobutane	0.80	0.611	337.8	1E+04	BC1	52
(Contd.)	0.80	0.818	342.1	1E+04	BC1	52
	0.80	0.910	342.4	1E+04	BC1	52
	0.80	1.020	345.2	1E+04	BC1	52
6. C_2H_3N/C_3H_3N	0.180	0.101	492.0	1E+06	BC1	54,55
Acetonitrile/	0.510	0.101	491.2	1E+06	BC1	54,55
acrylonitrile	0.810	0.101	489.0	1E+06	BC1	54,55
7. C_2H_6/C_3H_8	0.040	0.101	269.8	1E+05	BC1	59
Ethane/	0.140	0.101	275.1	1E+05	BC1	59
N-Propane	0.210	0.101	280.7	1E+05	BC1	59
	0.360	0.101	285.1	1E+05	BC1	59
	0.620	0.101	302.1	1E+05	BC1	59
	0.720	0.101	304.6	1E+05	BC1	59
	0.830	0.101	312.2	1E+05	BC1	59
	0.900	0.101	317.7	1E+05	BC1	59
8. C_2H_6/C_4H_{10}	0.060	0.101	271.4	1E+05	BC1	59
Ethane/	0.090	0.101	276.7	1E+05	BC1	59
N-Butane	0.170	0.101	282.3	1E+05	BC1	59
	0.650	0.101	333.9	1E+05	BC1	59
	0.740	0.101	348.1	1E+05	BC1	59
	0.880	0.101	360.1	1E+05	BC1	59
9. C_2H_6O/C_3H_8O	0.080	0.101	468.1	1E+05	BC1	11
Ethanol/	0.251	0.101	471.6	1E+05	BC1	11
N-Propanol	0.439	0.101	475.7	1E+05	BC1	11
	0.646	0.101	480.2	1E+05	BC1	11
	0.875	0.101	484.3	1E+05	BC1	11
10. C_2H_6O/C_6H_6	0.249	0.101	465.2	1E+01	CT2	28,29
Ethanol/	0.249	0.980	472.5	1E+01	CT2	28,29
Benzene	0.503	0.101	470.7	1E+01	CT2	28,29
	0.503	0.980	477.4	1E+01	CT2	28,29
	0.742	0.101	479.5	1E+01	CT2	28,29
	0.742	0.980	488.2	1E+01	CT2	28,29
	0.904	0.101	488.7	1E+01	CT2	28,29
	0.904	0.980	500.6	1E+01	CT2	28,29
11. $C_3H_6O/C_4H_{10}O$	0.350	0.101	474.8	1E+02	CT2	28,29
Acetone/	0.500	0.101	483.7	1E+02	CT2	28,29
N-Butanol	0.500	0.980	491.7	1E+01	CT2	29
	0.650	0.101	492.2	1E+02	CT2	28,29
	0.650	0.980	500.7	1E+01	CT2	29

Table 5: Limits of superheat of binary mixtures—Continued

Substance	X	P [MPa]	T [K]	J [nuclei/(cm^3•s)]	Method	Reference
12. C_3H_6O/C_6H_6	0.120	0.101	458.3	1E+01	CT2	29
Acetone/	0.120	0.980	468.3	1E+01	CT2	29
Benzene	0.220	0.101	463.6	1E+01	CT2	29
	0.220	0.980	471.7	1E+01	CT2	29
	0.350	0.101	469.6	1E+02	CT2	28
	0.350	0.980	477.2	1E+02	CT2	28
	0.500	0.101	473.6	1E+01	CT2	29
	0.500	0.980	482.3	1E+01	CT2	29
	0.503	0.101	476.6	1E+02	CT2	28
	0.503	0.980	485.0	1E+02	CT2	28
	0.750	0.101	484.8	1E+01	CT2	29
	0.750	0.980	494.8	1E+01	CT2	29
	0.900	0.101	493.2	1E+01	CT2	29
	0.900	0.980	507.6	1E+01	CT2,3	28,29
13. C_3H_8/C_4H_{10}	0.120	0.101	329.7	1E+05	BC1	59
N-Propane/	0.180	0.101	331.5	1E+05	BC1	59
2-Methyl-	0.260	0.101	334.7	1E+05	BC1	59
propane	0.320	0.101	337.0	1E+05	BC1	59
	0.450	0.101	341.5	1E+05	BC1	59
	0.560	0.101	344.3	1E+05	BC1	59
	0.660	0.101	349.2	1E+05	BC1	59
	0.800	0.101	353.2	1E+05	BC1	59
	0.930	0.101	357.1	1E+05	BC1	59
14. C_3H_8/C_4H_{10}	0.120	0.101	332.7	1E+06	BC1	61
N-Propane/	0.230	0.101	327.0	1E+06	BC1	61
N-Butane	0.380	0.101	347.7	1E+06	BC1	61
	0.570	0.101	355.7	1E+06	BC1	61
	0.650	0.101	359.4	1E+06	BC1	61
	0.780	0.101	369.5	1E+06	BC1	61
	0.920	0.101	372.6	1E+06	BC1	61
15. $C_3H_8O/C_4H_{10}O$	0.083	0.101	488.2	1E+04	BC1	11
N-Propanol/	0.259	0.101	493.8	1E+04	BC1	11
N-Butanol	0.450	0.101	498.7	1E+04	BC1	11
	0.656	0.101	504.4	1E+04	BC1	11
	0.880	0.101	509.2	1E+04	BC1	11
16. $C_4H_{10}O/N_2$	0.0042	0.402	419.4	1E+01	BC2	39,40
Ether/	0.0057	0.978	426.2	1E+01	BC2	38
Nitrogen	0.0067	1.557	433.5	1E+01	BC2	38
(Gas)	0.0092	2.239	443.2	1E+01	BC2	38
	0.0110	0.695	409.4	1E+01	BC2	39,40
	0.0139	1.273	426.2	1E+01	BC2	38
	0.0171	1.851	433.5	1E+01	BC2	38
	0.0191	1.102	419.4	1E+01	BC2	39,40
	0.0243	2.564	443.2	1E+01	BC2	38
	0.0250	1.710	426.2	1E+01	BC2	38
	0.0308	2.290	433.5	1E+01	BC2	38
	0.0431	3.012	443.2	1E+01	BC2	38

Table 5: Limits of superheat of binary mixtures—Continued

Substance	X	P [MPa]	T [K]	J [nuclei/(cm^3•s)]	Method	Reference
17. $C_4H_{10}O$/	0.086	0.101	511.6	1E+04	BCl	11
$C_5H_{10}O$	0.266	0.101	513.2	1E+04	BCl	11
N-Butanol/	0.458	0.101	518.7	1E+04	BCl	11
N-Pentanol	0.664	0.101	525.2	1E+04	BCl	11
	0.884	0.101	529.2	1E+04	BCl	11
18. C_5H_{12}/C_6H_{12}	0.130	0.101	436.7	1E+06	BCl	33
N-Pentane/	0.290	0.101	445.7	1E+06	BCl	33
Cyclo-	0.450	0.101	453.2	1E+06	BCl	33
hexane	0.600	0.101	463.2	1E+06	BCl	33
	0.730	0.101	473.2	1E+06	BCl	33
	0.850	0.101	483.2	1E+06	BCl	33
19. C_5H_{12}/C_6H_{14}	0.200	0.101	424.9	1E+04	BCl	42
N-Pentane/	0.250	0.101	426.8	1E+06	BCl	77
N-Hexane	0.400	0.101	432.5	1E+04	BCl	42
	0.500	0.101	435.8	1E+06	BCl	77
	0.600	0.101	439.4	1E+04	BCl	42
	0.800	0.101	446.5	1E+04	BCl	42
	0.900	0.101	449.2	1E+06	BCl	77
20. C_5H_{12}/C_7H_{16}	0.209	0.101	434.0	1E+04	BCl	12
N-Pentane/	0.209	0.653	441.3	1E+04	BCl	12
N-Heptane	0.209	1.204	453.2	1E+04	BCl	12
	0.209	2.032	463.9	1E+04	BCl	12
	0.442	0.101	451.4	1E+04	BCl	12
	0.442	0.377	456.8	1E+04	BCl	12
	0.442	0.653	462.0	1E+04	BCl	12
	0.442	0.929	465.9	1E+04	BCl	12
	0.442	1.204	470.3	1E+04	BCl	12
	0.442	1.480	475.3	1E+04	BCl	12
	0.442	1.756	478.4	1E+04	BCl	12
	0.442	2.032	482.0	1E+04	BCl	12
	0.442	2.308	486.7	1E+04	BCl	12
	0.442	2.583	489.9	1E+04	BCl	12
	0.745	0.101	471.5	1E+04	BCl	12
	0.745	0.239	473.7	1E+04	BCl	12
	0.745	0.377	476.8	1E+04	BCl	12
	0.745	0.653	481.9	1E+04	BCl	12
	0.745	0.929	486.0	1E+04	BCl	12
	0.745	1.204	491.1	1E+04	BCl	12
	0.745	1.480	494.4	1E+04	BCl	12
	0.745	1.756	498.9	1E+04	BCl	12
	0.745	2.032	501.6	1E+04	BCl	12
	0.745	2.308	508.4	1E+04	BCl	12
21. C_5H_{12}/C_8H_{18}	0.250	0.101	442.2	1E+05	BCl	12
N-Pentane/	0.250	0.653	451.7	1E+04	BCl	12
N-Octane	0.250	1.204	460.5	1E+04	BCl	12
	0.350	0.101	450.4	1E+06	BCl	61
	0.500	0.653	478.4	1E+04	BCl	12
	0.500	1.204	487.8	1E+04	BCl	12

Table 5: Limits of superheat of binary mixtures—Continued

Substance	X	P [MPa]	T [K]	J [nuclei/(cm^3•s)]	Method	Reference
21. C_5H_{12}/C_8H_{18} N-Pentane/ N-Octane (Contd.)	0.550	0.101	469.0	1E+06	BC1	61
	0.700	0.101	484.3	1E+06	BC1	61
	0.750	0.101	491.1	1E+04	BC1	12
	0.750	0.646	501.2	1E+04	BC1	12
	0.750	1.204	510.4	1E+04	BC1	12
	0.830	0.101	496.7	1E+06	BC1	61
22. $C_5H_{12}/C_{12}H_{26}$ N-Pentane/ N-Dodecane	0.150	0.101	450.8	1E+06	BC1	33
	0.290	0.101	473.2	1E+06	BC1	33
	0.450	0.101	510.0	1E+06	BC1	33
	0.600	0.101	532.4	1E+06	BC1	33
	0.730	0.101	560.0	1E+06	BC1	33
3. $C_5H_{12}/C_{16}H_{34}$ N-Pentane/N- Hexadecane	0.040	0.101	430.7	1E+06	BC1	22
	0.070	0.101	439.2	1E+06	BC1	22
	0.100	0.101	443.2	1E+04	BC1	12
	0.100	0.377	447.0	1E+04	BC1	12
	0.100	0.653	451.4	1E+04	BC1	12
	0.100	0.929	454.8	1E+04	BC1	12
	0.100	1.204	459.7	1E+04	BC1	12
	0.130	0.101	453.2	1E+06	BC1	22
	0.150	0.101	458.2	1E+06	BC1	22
	0.200	0.101	467.3	1E+04	BC1	12
	0.200	0.377	470.6	1E+04	BC1	12
	0.200	0.653	475.6	1E+04	BC1	12
	0.200	0.929	480.2	1E+04	BC1	12
	0.200	1.204	484.5	1E+04	BC1	12
	0.220	0.101	470.7	1E+06	BC1	22
	0.300	0.101	494.0	1E+04	BC1	12,33
	0.300	0.377	497.9	1E+04	BC1	12
	0.300	1.204	519.7	1E+04	BC1	12
	0.400	0.101	515.7	1E+06	BC1	33
	0.452	0.101	532.2	1E+06	BC1	33
	0.532	0.101	552.5	1E+06	BC1	33
	0.571	0.101	562.2	1E+06	BC1	33
24. C_6H_6/C_6H_{12} Benzene- Cyclo- hexane	0.045	0.310	498.4	1E+00	CT2	70
	0.110	0.310	497.4	1E+00	CT2	70
	0.200	0.101	493.1	1E+04	BC1	42
	0.226	0.310	495.8	1E+00	CT2	70
	0.340	0.310	493.7	1E+00	CT2	70
	0.400	0.101	490.4	1E+04	BC1	42
	0.489	0.310	493.6	1E+00	CT2	70
	0.600	0.101	489.8	1E+04	BC1	42
	0.608	0.310	492.5	1E+00	CT2	70
	0.765	0.310	492.1	1E+00	CT2	70
	0.800	0.101	489.7	1E+04	BC1	42
25. C_6H_6/C_6H_{14} Benzene/ N-Hexane	0.200	0.101	477.8	1E+04	BC1	42
	0.400	0.101	466.8	1E+04	BC1	42
	0.600	0.101	462.0	1E+04	BC1	42
	0.800	0.101	456.9	1E+04	BC1	42

Table 5: Limits of superheat of binary mixtures—Continued

Substance	X	P [MPa]	T [K]	J [nuclei/(cm^3·s)]	Method	Reference
26. C_6H_6/C_6H_{14}	0.200	0.101	459.8	1E+04	BC1	42
Cyclohexane/	0.400	0.101	466.9	1E+04	BC1	42
N-Hexane	0.600	0.101	473.4	1E+04	BC1	42
	0.800	0.101	481.6	1E+04	BC1	42
27. C_6H_{14}/C_7H_{16}	0.250	0.101	463.2	1E+07	BC1	73
N-Hexane/	0.500	0.101	471.1	1E+07	BC1	73
N-Heptane	0.750	0.101	479.3	1E+07	BC1	73

Table 6: Limits of superheat of ternary mixtures

Substance	X(C_2)	X(C_3)	P [MPa]	T [K]	J	Method	Reference
1. $C_2H_6/C_3H_8/$	0.806	0.155	0.101	278.4-281.2	1E+05	BC1	59
C_4H_{10}	0.806	0.073	0.101	280.8-283.4	1E+05	BC1	59
Ethane/	0.092	0.811	0.101	324.0-329.8	1E+05	BC1	59
N-Propane/	0.100	0.771	0.101	326.0-331.0	1E+05	BC1	59
N-Butane	0.235	0.433	0.101	324.8-344.2	1E+05	BC1	59
	0.113	0.652	0.101	329.4-334.8	1E+05	BC1	59
	0.160	0.299	0.101	337.8-354.4	1E+05	BC1	59
	0.076	0.403	0.101	342.4-353.0	1E+05	BC1	59
	0.135	0.160	0.101	344.6-355.8	1E+05	BC1	59

7. Nomenclature

G defined as $\Delta\Phi^*/KT$
J bulk nucleation rate (nuclei/cm^3·s)
k Boltzmann constant
k_f molecular evaporation rate (molecules/s)
m molecular mass
n unit outward normal to nucleus surface (Fig. 3)
N_0 number density of single activated molecules
P gas pressure in nucleus
P_o ambient pressure
P_s saturation pressure at T_k
r radius of nucleus
R gas constant
T temperature
T_c critical temperature
T_k kinetic limit of superheat at P_0 [Eq. (4)]
T_r reduced temperature ($= T/T_c$)
T_s saturation temperature at P_o [Eq. (2)]
T_t thermodynamic limit of superheat at P_0
T' minimum liquid temperature below which ambient pressure around nucleus is extensive (Fig. 3)
v_l liquid specific volume
α_l liquid thermal diffusivity
σ surface tension of superheat liquid with respect to its own vapor
σ_{12} interfacial tension between test and field liquids

8. Acknowledgments

The author thanks Mr. Mahmoud Fatehi for assistance in carrying out the extensive literature search that formed a major effort of the present work. He also thanks Professor Robert E. Apfel of Yale University for several constructive comments. This work was supported by the Office of Basic Energy Sciences of the Department of Energy through National Bureau of Standards—Office of Standard Reference Data under Grant No. NB82NADA3001, with Dr. Howard J. White, Jr. as project monitor. Additional support was received from the National Science Foundation through Grant No. CPE-8106348 (Dr. Robert M. Wellek, Program Director). This support is greatly appreciated.

9. References

Many more papers exist than were included in this reference list on the subject of homogeneous nucleation in liquids. Those sources dealing exclusively with theoretical methods and measurement of unrelated properties of superheated liquids (e.g., specific volume, sound speed, compressibility, etc.) were not of direct relevance to the intent of the present work. Most of the literature in the final listing contained superheat limit data of direct relevance to this work, or contained information which bore on the criteria for inclusion of these data in Tables 4–6.

[1]R. E. Apfel, Nature (London) Phys. Sci. **238**, 63 (1972).
[2]R. E. Apfel, Nature (London) Phys. Sci. **233**, 119 (1971).
[3]R. E. Apfel, J. Acoust. Soc. Am. **49**, 145 (1971).
[4]R. E. Apfel, Sci. Am. **227**, 58 (1972).
[5]R. E. Apfel and J. P. Harbison, J. Acoust. Soc. Am. **57**, 1371 (1975).
[6]R. E. Apfel, Technical Memorandum No. 62, Acoustics Research Laboratory, Harvard University, Cambridge, MA (1970).
[7]R. E. Apfel, J. Chem. Phys. **54**, 62 (1971).
[8]R. E. Apfel, J. Appl. Phys. **48**, 2077 (1977).
[9]C. T. Avedisian and R. P. Andres, J. Colloid Interface Sci. **64**, 438 (1978).
[10]C. T. Avedisian and I. Glassman, Int. J. Heat Mass Transfer **24**, 695 (1981).
[11]C. T. Avedisian and J. R. Sullivan, Chem. Eng. Sci. **39**, 1033 (1984).
[12]C. T. Avedisian and I. Glassman, J. Heat Transfer **103**, 272 (1981).
[13]C. T. Avedisian, J. Heat Transfer **105**, 750 (1982).
[14]V. G. Baidakov, V. P. Skripov, and A. M. Kaverin, Sov. Phys. JETP **38**, 557 (1974).
[15]V. G. Baidakov and V. P. Skripov, Russ. J. Phys. Chem. **56**, 499 (1982).
[16]G. S. Bankoff, in *Proceedings of the 6th International Heat Transfer Conference* (Hemisphere, Toronto, 1978), p. 355.
[17]D. K. Basu and D. B. Sinha, Indian J. Phys. **42**, 198 (1968).
[18]J. W. Beams, Phys. Fluids **1**, 1 (1959).
[19]B. L. Beegle, M. Modell, and R. C. Reid, AIChE J. **20**, 1200 (1974).
[20]M. Berthelot, Ann. Chem. (Phys.) **30**, 232 (1850).
[21]F. Blake, Technical Memorandum No. 9, Acoustics Research Laboratory, Harvard University, Cambridge, MA (1949).
[22]M. Blander, D. Hengstenberg, and J. L. Katz, J. Phys. Chem. **75**(23), 3613 (1971).
[23]M. Blander and J. L. Katz, AIChE J. **21**, 833 (1975).
[24]L. J. Briggs, J. Appl. Phys. **21**, 721 (1950).
[25]L. J. Briggs, J. Chem. Phys. **19**, 970 (1951).
[26]L. C. Brodie, D. N. Sinha, J. S. Semura, and C. E. Sanford, J. Appl. Phys. **48**, 2882 (1982).
[27]M. G. Buivid and M. V. Sussman, Nature **275**, 203 (1978).
[28]N. N. Danilov and Ye. N. Sinitsyn, Heat Transfer Sov. Res. **12**, 71 (1980).
[29]N. N. Danilov, Ye. N. Sinitsyn, and V. P. Skripov, "Spontaneous Vapor Nuclei Formation in Superheated Liquid Solutions," in *Gidrodinamika i Teploobmen v Energeticheskih Ustanovkakh* (Academy of Sciences of the USSR, 1975), p. 3.
[30]A. Ye. Dianov, V. G. Mal'tsev, V. G. Baydakov, and V. Skripov, Heat Transfer Sov. Res. **12**, 75 (1980).
[31]M. L. Dufour, C. R. Acad. Sci. **52**, 986 (1861).
[32]M. L. Dufour, C. R. Acad. Sci. **53**, 846 (1861).
[33]J. G. Eberhart, W. Kremsner, and M. Blander, J. Colloid Interface Sci. **50**, 369 (1975).
[34]J. G. Eberhart, E. J. Hathaway, and M. Blander, J. Colloid Interface Sci. **44**, 389 (1973).
[35]G. V. Ermakov and V. P. Skripov, Russ. J. Phys. Chem. **43**, 1242 (1969).
[36]G. V. Ermakov and V. P. Skripov, Russ. J. Phys. Chem. **41**, 39 (1962).
[37]G. V. Ermakov, V. G. Baidakov, and V. P. Skripov, Russ. J. Phys. Chem. **47**, 582 (1973).
[38]T. W. Forest and C. A. Ward, ASME Paper No. 77-HT-58 (1977).
[39]T. W. Forest and C. A. Ward, J. Chem. Phys. **66**, 2322 (1977).
[40]T. W. Forest and C. A. Ward, J. Chem. Phys. **69**, 2221 (1978).
[41]J. W. Gibbs, *The Collected Works of J. Willard Gibbs* (Longmans, Green, New York, 1928), Vol. 1.
[42]B. S. Holden and J. L. Katz, AIChE J. **24**, 260 (1978).
[43]B. S. Holden, M.S. thesis (Clarkson College of Technology, Potsdam, NY, 1976).
[44]J. Hord, R. B. Jacobs, C. C. Robinson, and L. L. Sparks, J. Eng. Power **86**, 485 (1964).
[45]T. J. Jarvis, M. D. Donohue, and J. L. Katz, J. Colloid Interface Sci. **50**, 359 (1975).
[46]W. M. Jones, G. D. N. Overton, and D. H. Trevena, J. Phys. D **14**, 1283 (1981).
[47]F. B. Kenrick, C. S. Gilbert, and K. L. Wismer, J. Phys. Chem. **28**, 1297 (1924).
[48]P. O. Biney, W. Dong, and J. H. Lienhard, paper presented at the 23rd ASME/AIChE National Heat Transfer Conference, 1985 (to be published).
[49]J. H. Lienhard and A. H. Karimi, J. Heat Transfer **100**, 492 (1978).
[50]P. L. Marston, J. Low Temp. Phys. **25**, 383 (1976).
[51]G. R. Moore, AIChE J. **5**, 458 (1959).
[52]Y. Mori, K. Hijikata, and T. Nagatani, Int. J. Heat Mass Transfer **19**, 1153 (1976).
[53]K. Nishigaki and Y. Saji, Jpn. J. Appl. Phys. **20**, 849 (1981).
[54]J. R. Patrick-Yeboah, Ph. D. thesis (MIT, Cambridge, MA, 1979).
[55]J. R. Patrick-Yeboah and R. C. Reid, Ind. Eng. Chem. Fundam. **20**, 315 (1981).
[56]P. A. Pavlov and V. P. Skripov, High Temp. (USSR) **8**, 540 (1970).
[57]D. Yu. Peng and D. B. Robinson, Ind. Eng. Chem. Fundam. **15**, 59 (1976).
[58]H. T. Pham, S. M. thesis (MIT, Cambridge, MA, 1977).
[59]W. Porteous and M. Blander, AIChE J. **21**, 560 (1975).
[60]R. C. Reid, Adv. Chem. Eng. **12**, 105 (1983).
[61]T. A. Renner, G. H. Kucera, and M. Blander, J. Colloid Interface Sci. **52**, 319 (1975).
[62]J. E. Shepherd and B. Sturtevant, J. Fluid Mech. **21**, 379 (1982).
[63]D. B. Sinha and A. K. Jalaluddin, Indian J. Phys. **35**, 311 (1961).
[64]D. N. Sinha, Ph.D. thesis (Portland State University, Portland, OR, 1982).
[65]D. H. Sinha, J. S. Semura, and L. C. Brodie, Phys. Rev. A **26**, 1048 (1982).
[66]Ye. N. Sinitsyn and N. N. Danilov, Heat Transfer Sov. Res. **12**, 66 (1980).
[67]Ye. N. Sinitsyn and V. P. Skripov, Russ. J. Phys. Chem. **42**, 440 (1968).
[68]Ye. N. Sinitsyn and V. P. Skripov, Pribory Tekh. Eksp. **4**, 178 (1966).
[69]Ye. N. Sinitsyn and V. P. Skripov, Ukr. Phys. J. **12**, 100 (1967).
[70]E. N. Sinitsyn, N. N. Danilov, and V. P. Skripov, Teplofizika **425**, 22 (1971).
[71]V. P. Skripov and G. V. Ermakov, Russ. J. Phys. Chem. **38**, 208 (1964).
[72]V. P. Skripov and P. A. Pavlov, High Temp. (USSR) **8**, 782 (1970).
[73]V. P. Skripov and V. L. Kukushkin, Russ. J. Phys. Chem. **35**, 139 (1961).
[74]V. P. Skripov, V. G. Baidakov, and A. M. Kaverin, Phys. Sci. **95 A**, 169 (1979).
[75]V. P. Skripov, P. A. Pavlov, and E. N. Sinitsyn, High Temp. (USSR) **3**, 670 (1965).
[76]V. P. Skripov and Ye. N. Sinitsyn, Russ. J. Phys. Chem. **42**, 167 (1968).
[77]V. P. Skripov, *Metastable Liquids* (Wiley, New York, 1974).
[78]V. P. Skripov and G. V. Ermakov, Russ. J. Phys. Chem. **37**, 1047 (1963).
[79]J. R. Sullivan, M. Eng. project report (Cornell University, Ithaca, NY, 1982).
[80]H. N. V. Temperley, Proc. Phys. Soc. London **49**, 203 (1947).
[81]D. H. Trevena, Contemp. Phys. **17**, 109 (1976).
[82]S. J. D. Van Stralen and R. Cole, *Boiling Phenomena* (Hemisphere, New York, 1979), Vol. 1, Chap. 4.
[83]V. E. Vinogradov, E. N. Sinitsyn, and V. P. Skripov, *Art. Acad. Sci. White Russ. SSR* (Physics-Energetics Science Series), No. 1 (UDC 536.423.18) (1977), p. 17.
[84]H. Wakeshima and K. Takata, J. Phys. Soc. Jpn. **13**, 1398 (1958).
[85]K. L. Wismer, J. Phys. Chem. **26**, 301 (1922).